

HOSTED BY



ELSEVIER

Contents lists available at ScienceDirect

China University of Geosciences (Beijing)

Geoscience Frontiers

journal homepage: www.elsevier.com/locate/gsf

Research paper

The Gondwana Orogeny in northern North Patagonian Massif: Evidences from the Caita Có granite, La Seña and Pangaré mylonites, Argentina

Daniel A. Gregori^{a,*}, Bernhardt Saini-Eidukat^b, Leonardo Benedini^a, Leonardo Strazzere^a, Mercedes Barros^a, José Kostadinoff^c

^a Cátedra de Geología Argentina, Departamento de Geología, Universidad Nacional del Sur and INGEOSUR, San Juan 670, 8000 Bahía Blanca, Argentina

^b Department of Geosciences, North Dakota State University, Fargo, ND 58105-5517, USA

^c Cátedra de Campos Gravitacionales, Departamento de Física, Universidad Nacional del Sur, Argentina

ARTICLE INFO

Article history:

Received 30 September 2014

Received in revised form

16 May 2015

Accepted 1 June 2015

Available online xxx

Keywords:

Gondwana Orogeny

Northern Patagonia

Foliated granite

Mylonites

Argentina

ABSTRACT

Structural analyses in the northern part of the North Patagonia Massif, in the foliated Caita Có granite and in La Seña and Pangaré mylonites, indicate that the pluton was intruded as a sheet-like body into an opening pull-apart structure during the Gondwana Orogeny. Geochronological studies in the massif indicate a first, lower to middle Permian stage of regional deformation, related to movements during indentation tectonics, with emplacement of foliated granites in the western and central areas of the North Patagonian Massif. Between the upper Permian and lower Triassic, evidence indicates emplacement of undeformed granitic bodies in the central part of the North Patagonian Massif. A second pulse of deformation between the middle and upper Triassic is related to the emplacement of the Caita Có granite, the development of mylonitic belts, and the opening of the Los Menucos Basin. During this pulse of deformation, compression direction was from the eastern quadrant.

© 2015, China University of Geosciences (Beijing) and Peking University. Production and hosting by Elsevier B.V. This is an open access article under the CC BY-NC-ND license (<http://creativecommons.org/licenses/by-nc-nd/4.0/>).

1. Introduction

The North Patagonian Massif of Argentina occupies most of the northern Patagonia. It is bounded by Jurassic–Cretaceous basins and covered by Tertiary–Quaternary sequences (Fig. 1). The Jurassic–Cretaceous Neuquén Basin and the Limay lineament appear westwards and northwards of the massif, whereas the Jurassic–Cretaceous Cañadón Asfalto and San Jorge basins together with the Gastre and Comallo lineaments (Coira et al., 1975) form its south and southwestern border. The Huincul fault zone is believed to represent the northern edge of the North Patagonian Massif (Gregori et al., 2008, 2013). Eastwards the border is located in the marine platform.

In the North Patagonian Massif there are outcrops of Neoproterozoic–Cambrian metamorphic rocks (Pampean Orogeny), Ordovician to Devonian marine sequences (Famatinian Orogeny),

Permo-Triassic intrusives (Gondwana Orogeny) and Jurassic volcanic complexes (Patagonian Orogeny). Cretaceous and Tertiary times (Andean Orogeny) are widely represented by nearly horizontal sedimentary sequences and volcanic rocks that cover older units.

The Pampean rocks outcrop mainly in the eastern part of the Massif and appear as positive Bouguer anomalies (Kostadinoff et al., 2005; Gregori et al., 2008, 2013). The rocks display characteristics of sequences deposited in marine calcareous platforms, such those identified in central and northern Argentina (González et al., 2002a, 2011).

The Famatinian Orogeny in northern Patagonia is represented by intrusive and sedimentary rocks, similar to the Sierras Pampeanas of central Argentina. The marine basin, represented by the Sierra Grande Formation (Ordovician–Devonian) shares the same lithology and fossil remains with the rocks on the Sierra de la Ventana Basin (Cambrian–Devonian), located 500 km northeastwards (Gregori et al., 2013). Both depocenters were deformed in the upper Devonian–lower Carboniferous by the Chanic diastrophic phase.

* Corresponding author. Tel.: +54 291 4515901x3031; fax: +54 291 4595148.

E-mail address: usgregor@criba.edu.ar (D.A. Gregori).

Peer-review under responsibility of China University of Geosciences (Beijing).

<http://dx.doi.org/10.1016/j.gsf.2015.06.002>

1674-9871/© 2015, China University of Geosciences (Beijing) and Peking University. Production and hosting by Elsevier B.V. This is an open access article under the CC BY-NC-ND license (<http://creativecommons.org/licenses/by-nc-nd/4.0/>).

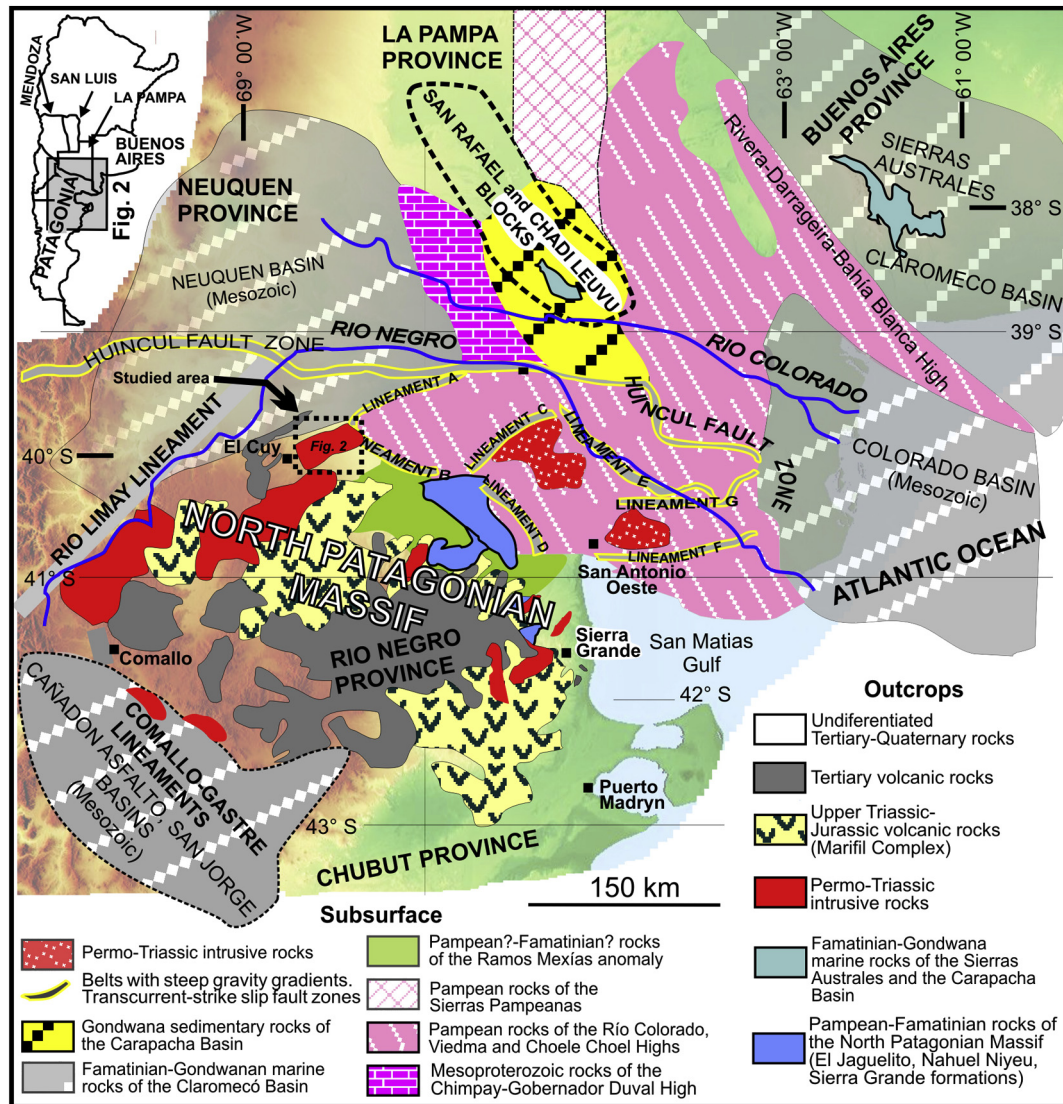


Figure 1. Regional map of northern Patagonia showing also the southern part of Buenos Aires and La Pampa provinces. The eastern part of Neuquén Province and the northern part of Chubut Province are included. The Jurassic–Cretaceous basins (Neuquén, Colorado and Cañadón Asfalto) are the borders of the North Patagonian Massif. Major geological units depicted, as well as steep gravity gradient belts. Subsurface geological interpretations are shown. See location of Fig. 2.

A substantial portion of the outcrops, mainly in the northern domain of the North Patagonian Massif, are intrusive and volcanic rocks belonging to the Gondwana and Patagonian orogenies (Fig. 1). Nearly all Permian plutonic-volcanic complexes initiate with I-type intrusives that quickly pass to S-type granites (Llambías and Rapela, 1984; Rapela and Caminos, 1987; Rapela and Llambías, 1985; Grecco et al., 1994 and references therein). The Triassic to Jurassic volcanic sequence that capped the plutonic-volcanic complexes includes pyroclastic and volcanoclastic sequences. Different to the Permian events which are developed as isolated magmatic centers, the Triassic to Jurassic volcanic sequences cover wide extension in northern Patagonia.

The origin of the Permian plutonic-volcanic complexes is not completely understood, partly due to an almost flat relief that prevents the recognition of intrusive relations, as well as relations with regional structures; and also to the scarcity of detailed mapping to understand its stratigraphic architecture.

The absence of detailed geochemical studies, as well as U-Pb ages in most of the intrusive complexes preclude to imagine a scenario for the origin of Permian intrusive rocks. Geochemical data of major

and some trace elements, as well as radiometric dating, were provided by Rapela and Llambías (1985) in La Esperanza, Rapela and Caminos (1987) in Navarrete area, Rapela et al. (1992) in the Gastre area, Grecco et al. (1994) and Grecco and Gregori (2011) in the Pailemán area, and Pankhurst et al. (2006) all around the North Patagonian Massif. However, a deep discussion about the origin of these bodies was not carried out by these authors.

One of the most cited hypotheses about the origin of the Permian plutonic-volcanic complexes belongs to Ramos (1984, 2008), who considered the rocks as subduction-related, due to the approaching of the so-called Patagonia Terrane to the southern margin of the Gondwana supercontinent.

This hypothesis considered Patagonia as an autochthonous block to Gondwana supercontinent until the Devonian when the first separates about 1000 km from Gondwana. By the Carboniferous, the Patagonia Terrane returned to the Gondwana southern margin. According to Ramos (1984, 2008), the contact between Patagonia and Gondwana started during the Carboniferous, but collision, deformation and uplift took place in early Permian times. The collision produced deformation in a foreland area located more

than 480 km northeastwards (Sierras Australes of Buenos Aires Province). Previously to the collision, the oceanic crust must be subducted below the Patagonian crust generating a magmatic arc that crosses northern Patagonia in a west-east direction for more than 500 km.

However, the supposition on the subduction-related origin of the intrusive complex is not based on petrologic, geochemical or isotopic evidences, but on the hypothesis that the alleged subduction and collision is the generator of the magmatic arc in the North Patagonian Massif and deformation in Sierras Australes of the Buenos Aires Province.

The research by Pankhurst et al. (2006) provided a large amount of geochemical and isotopic data on the magmatic rocks of northern Patagonia that lead to those authors to discard the existence of the magmatic arc invoked by Ramos (1984, 2008).

During the time of approaching of the Patagonia Terrane to Gondwana, a Carboniferous accretionary prism with emplaced oceanic crust must be formed. This suture zone should be located in the active northern margin of the Patagonia Terrane, which correspond to an area located north of the North Patagonian Massif, actually cover by Tertiary–Quaternary rocks.

To locate this supposed suture zone, geophysical studies were carried out by Kostadinoff et al. (2005) and Gregori et al. (2008, 2013). The results confirm the absence of ultramafic rock belts located in the area of the supposed suture. Moreover, rocks that can be assigned to an accretionary prism were never found in northern Patagonia or Sierras Australes of the Buenos Aires Province.

A remarkable deformation occurred during the Gondwana Orogeny in northern Patagonia. It is represented by regional shear bands, foliated granites, mylonite strips and folding and faulting of the Ordovician–Devonian marine sequences (Gregori et al., 2008, 2013).

The results of the geophysical studies indicate the existence of curvilinear belts with steep gravity gradients in subsurface. The more notable and also recognized in surface is the Huincul fault zone that crosses northern Patagonia in a west-east direction from the Andes to the Atlantic coast (Fig. 1).

According to Gregori et al. (2008, 2013) dextral movement along the E–W-trending Huincul Fault Zone resulted in block collage, W–NW crustal translations, and counterclockwise rotation of large crustal blocks belonging to the North Patagonia Massif. The indentation of these blocks within the North Patagonia Massif resulted in tectonic escape of the surrounding blocks, which can explain the diversity of stress directions during the Gondwana Orogeny.

An effect of this deformation was a dextral displacement of about 300 km in a W–E direction of the Ordovician–Devonian Sierras Australes of the Buenos Aires Province and Sierra Grande depocenters of through the Huincul Fault zone (Gregori et al., 2013).

Other belts of steep gravity gradients in northern Patagonia (Gregori et al., 2013) are coincident or follow the trace of shear zones and mylonitic belts active during Gondwana times. Most granitic bodies located in the eastern part of the North Patagonian Massif (La Laguna, Peñas Blanca, María Teresa, Tapera stocks) were deformed and foliated during their emplaced along shear zones in the Gondwana Orogeny and their geochemistry do not show subduction-related signatures (Gregori et al., 2008).

The different interpretations on the origin of the Permo-Triassic intrusives make necessary a detailed study about the style of emplacement of the Gondwana foliated granites. We present a more precise age of the foliated granite in the northern central part of the North Patagonian Massif, as well as, its relationships with the mylonitic belts. We would like to recognize if the escape tectonic model proposed by Gregori et al. (2008) can be applicable in this sector in order to understand the style of deformation and the effects of the Gondwana Orogeny.

2. Paleozoic geology of the northern North Patagonian Massif

2.1. Pampean Orogeny

Along the northern border of the North Patagonian Massif (Fig. 1), there are outcrops of low- and medium-grade metamorphic rocks (phyllite, metasandstone, marl, amphibolite and limestone) of the El Jagüelito, Colo Niyeu and Nahuel Niyeu formations and the Mina Gonzalito Complex (Ramos, 1975; Caminos, 1983; Labudía and Bjerg, 1994; González et al., 2002a). All of these belong to the Pampean Orogeny (late Proterozoic–middle Cambrian), typical of the northern and central part of Argentina (Tickj et al., 2002; Rapela et al., 2003; Gregori et al., 2008). Radiometric dating of Pampean metamorphic rocks of central Argentina indicates ages of 500, 515, 518, 526 and 533 Ma (González et al., 2002b; Chernicoff et al., 2008). In the Valcheta area (North Patagonian Massif) detrital zircons indicate an age of ~535 Ma for the El Jagüelito Formation, ~515 Ma for the Nahuel Niyeu Formation and 605 ± 7 Ma and 535–540 Ma for the Mina Gonzalito Complex (Pankhurst et al., 2006). Minor components in the Mina Gonzalito sample (Pankhurst et al., 2006), older than ~1000–1200 Ma could be related to a provenance from the areas immediately eastward, including the Río de la Plata and Kalahari cratons.

The subsurface extension of the Pampean rocks was established by Kostadinoff and Labudía (1991), Kostadinoff et al. (2005), and Gregori et al. (2008, 2013) by means of gravity studies (Fig. 1). The overall distribution of the gravity anomalies is in a N–S direction, from San Luis (central Argentina) to the Río Negro Province. In the northern and eastern part of the Río Negro, the Río Colorado, Choele Choele and Viedma residual anomalies range from -27 to 15 mGal. These values are similar to those recorded in the San Luis Province and according to these evidence, the marine basin, known as the “Puncoviscana Basin” (González et al., 2002a) extended between northern Argentina and the North Patagonian Massif during late Proterozoic–middle Cambrian times.

2.2. Famatinian Orogeny

Ordovician–Devonian rocks (Famatinian Orogeny) are scarce in northern Patagonia and are related to basins in the Sierra Grande and Gastre areas (Fig. 1). The Sierra Grande Formation shares similar lithologies, paleofauna, and deformation characteristics with the Ventana Group of the Sierra de la Ventana in the Buenos Aires Province. These similarities suggest that both units were deposited in the same basin, part of which is now buried underneath the Mesozoic Colorado Basin (Fig. 1). Both the Claromecó and Sierra Grande Basin can be successfully correlated with the Table Mountain and Bokkeveld groups within the Cape Fold Belt of South Africa, as well as, the sedimentary successions in the Malvinas (Falkland) Islands and the Ellsworth mountains in Antarctica (Keidel, 1916, 1925; Buggisch, 1987). The Ventana Group and the Sierra Grande Formation are formed by a 1500 m thick sequence that includes minor conglomerate, quartzite and pelite deposited in a marine platform environment.

In the North Patagonian Massif (Fig. 1), the Famatinian Orogeny is also represented by intrusive rocks. These include the Arroyo Salado granodiorite, Punta Sierra granite, Hiparsa granite, El Molino and Laguna Medina plutons. Ages vary between 483 ± 22 and 318 ± 28 Ma using Rb/Sr dating (Varela et al., 1997, 1998). U/Pb dating indicates that the magmatism is restricted to the lower Ordovician (476–472 Ma) according to the data of Varela et al. (1997, 1998), Pankhurst et al. (2006), and González et al. (2008).

Therefore, the timing of the Famatinian Orogeny in the North Patagonian Massif is constrained to the lower Ordovician–Devonian. These ages are similar to those recorded in northern and

central Argentina. The evidences imply the continuity of the Famatinian Belt into northern Patagonia as suggested by Pankhurst et al. (2001) and other authors.

The subsurface extension of the Famatinian rocks is practically unknown due to the scarcity of the outcrops and to the small density contrast between the Famatinian and Gondwanan sedimentary and igneous rocks. One exception is the Sierra Grande Basin, characterized by several negative gravity anomalies (-30 , -20 mGal), that extend along the Atlantic coast south of 44°S (Kostadinoff and Schillizzi, 1988, 1996; Kostadinoff and Gelós, 1994).

2.3. Gondwana Orogeny

This is represented by igneous rocks with ages between Carboniferous and Triassic. The Gondwana igneous rocks are widely represented in the North Patagonian Massif by two separate belts oriented SSW–NNE, and NW–SE, respectively (Fig. 1). The first, located in the western area of this region, include the foliated Mamil Choique granitoids. K/Ar and U/Pb radiometric dating (SHRIMP and TIMS of whole in zircon) in this unit and similar (Paso Flores tonalite, Comallo granodiorite, Yuncón granite, Loma Miranda tonalite and Piedra del Aguila granite), yield ages between 386.6 ± 5.4 and 272.4 ± 2.2 Ma (Varela et al., 2005; Pankhurst et al., 2006). These rocks were assigned to a magmatic arc developed on continental crust by Varela et al. (2005).

In the northern tip of this belt the outcrop of Caita Có granite (studied in this paper) dated 224 ± 5 Ma (U/Pb, zircon LA-ICP-MS; Saini-Eidukat et al., 2004). The non-foliated granites of this belt (Lipetrén, Chasicó, Fita Ruin, Cayupil, Palenquenyue, La Esperanza Plutonic Complex, Dos Lomas Plutonic-Volcanic Complex and Alessandrini Complex), yield ages between 273 and 207 Ma (Rb/Sr, U/Pb in zircon using SHRIMP and LA-ICP-MS). The results point to lower Permian to upper Triassic ages according to the data of Llambías and Rapela (1984), Dalla Salda et al. (1991), Rapela et al. (1991, 1996), Saini-Eidukat et al. (2004) and Pankhurst et al. (2006).

The second, NW–SE trending belt, is represented in the northern and eastern part of the North Patagonian Massif (Fig. 1) by foliated intrusive bodies including the Treneta granite (305 ± 31 Ma U/Pb zircon, 244 ± 9 Ma Rb/Sr), Tardugno granodiorite (300 ± 6 Ma U/Pb zircon), Puesto Peynecura granite (281 ± 29 Ma U/Pb zircon),

Puesto Peynecura granodiorite (244 ± 14 Ma U/Pb zircon), Tapera granite, María Teresa granite, Peñas Blancas and La Laguna granites (Basei et al., 2002), indicating Upper Carboniferous to Lower Triassic ages.

The non-foliated granites include the Navarrete and Treneta complexes (Rapela and Caminos, 1987, 283 ± 3 Ma; Pankhurst et al., 2006), Arroyo Pailemán and Arroyo Tembrao stocks (268 ± 3 Ma, Rb/Sr; Grecco et al., 1994), San Martín granite (ca. 267 Ma, U/Pb, zircon, SHRIMP; Pankhurst et al., 2006), La Verde granite (253 ± 9 Ma; Linares, 1994 in Busteros et al., 1998), and Laguna Medina granodiorite (Varela et al., 2009, get an age of Rb/Sr of 260 ± 3 Ma.). The radiometric dating of these units ranges between 273 ± 2 and 246 ± 2 Ma (U/Pb, zircon, SHRIMP; Pankhurst et al., 2006). The results indicate the existence of a notable magmatism, similar in age to that widely recognized in central western Argentina (Fig. 1).

3. Geology of El Cuy and Caita Có regions

Bjerg et al. (1998) reported the preliminary stratigraphy of the eastern area of the El Cuy region. The older rocks (phyllites and schists) that crop out north of Estancia Pangaré were assigned to the Eopaleozoic Coli Niyue Formation (Labudía and Bjerg, 1994). They were intruded by foliated leucogranites of the late Ordovician–early Silurian Mamil Choique Formation (Dalla Salda et al., 1994), in the Estancias La Seña and Pangaré area (Figs. 2, 3, 6 and 7).

Granites and aplitic dikes which were correlated with the La Esperanza Plutonic Complex (Llambías and Rapela, 1984) located 100 km SW, intruded both units, whereas dacitic-rhyolitic ignimbrites comparable with the Dos Lomas Plutonic Volcanic Complex (upper part of La Esperanza Complex) overlie the granites. Both units represent the Permo-Triassic magmatism.

New field work, accompanied with preliminary radiometric dating (Saini-Eidukat et al., 1999, 2004; Gregori et al., 2000) in the Estancias La Seña and Pangaré area (Fig. 2) demonstrated that the units previously assigned to the La Esperanza Plutonic Complex and the Dos Lomas Plutonic Volcanic Complex are indeed Late Triassic to Early Jurassic. Cretaceous continental and marine sedimentary sequences cover the igneous rocks, whereas basaltic volcanic rocks constitute the late Tertiary.

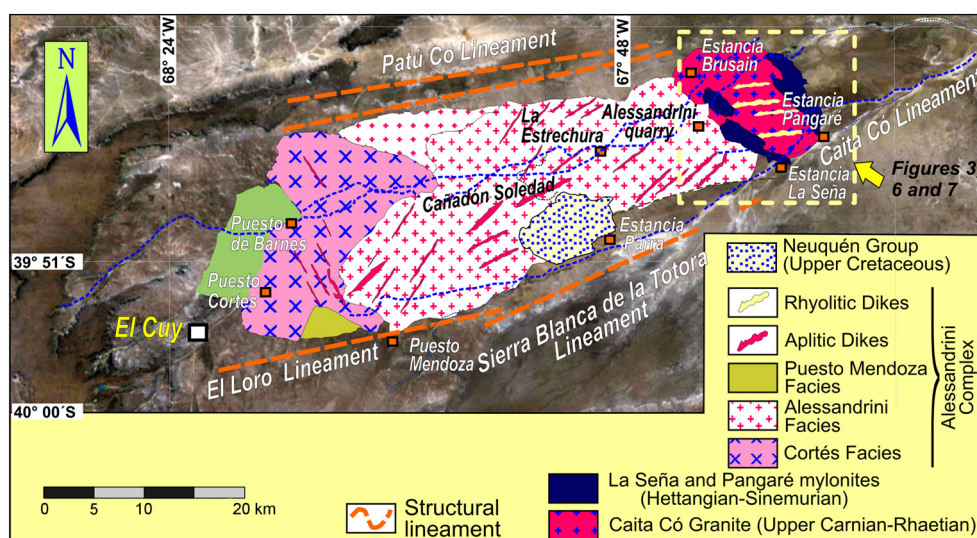


Figure 2. Geological sketch of the area located east of El Cuy, Patu' Có and El Loro-Sierra Blanca de la Totorá lineaments border the outcrops of the igneous rocks. Location of Figs. 3, 6 and 7 is shown. Location of Caita Có granite, La Seña and Pangaré mylonites are displayed.

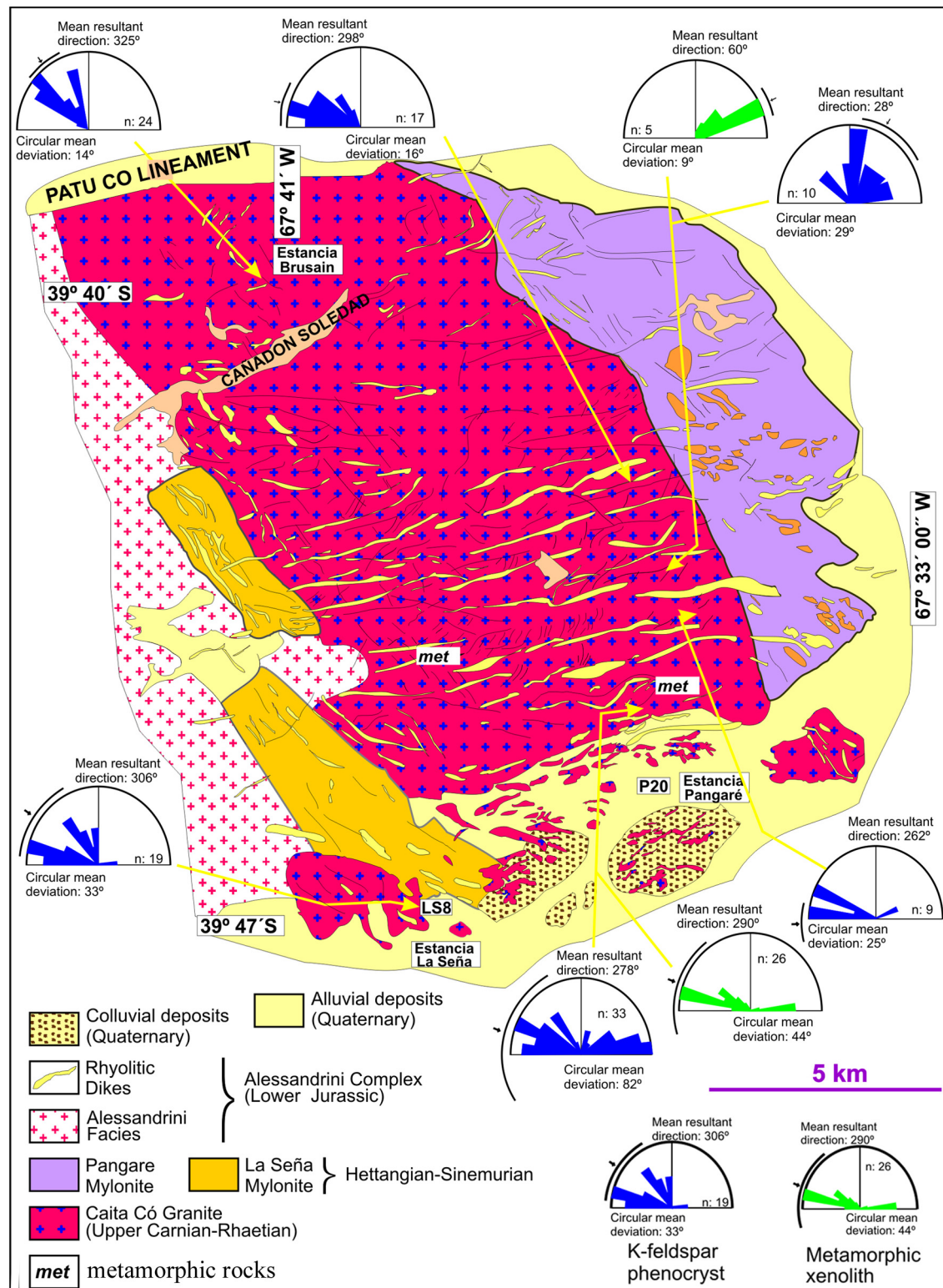


Figure 3. Geological map of the Pangaré and La Seña area showing the location of Caíta Có granite, Alessandrini Complex and La Seña and Pangaré mylonites. Frequency diagrams of orientation of the K-feldspar phenocryst and metamorphic xenoliths in the Caíta Có granite are displayed.

4. Geology of La Seña-Pangaré area

Field mapping in the Estancias La Seña and Pangaré area, together with sampling, structural measurements and geochronology allow us to recognize a foliated granite body and two belts of mylonites.

The eastern one, named here Pangaré Mylonite, extends from Sierra Blanca de la Totorá Lineament to Patu Có Lineament in the area of Estancia Pangaré. Northwards and southwards is covered by Tertiary and Quaternary units making it difficult to establish its real dimensions (Figs. 2 and 3).

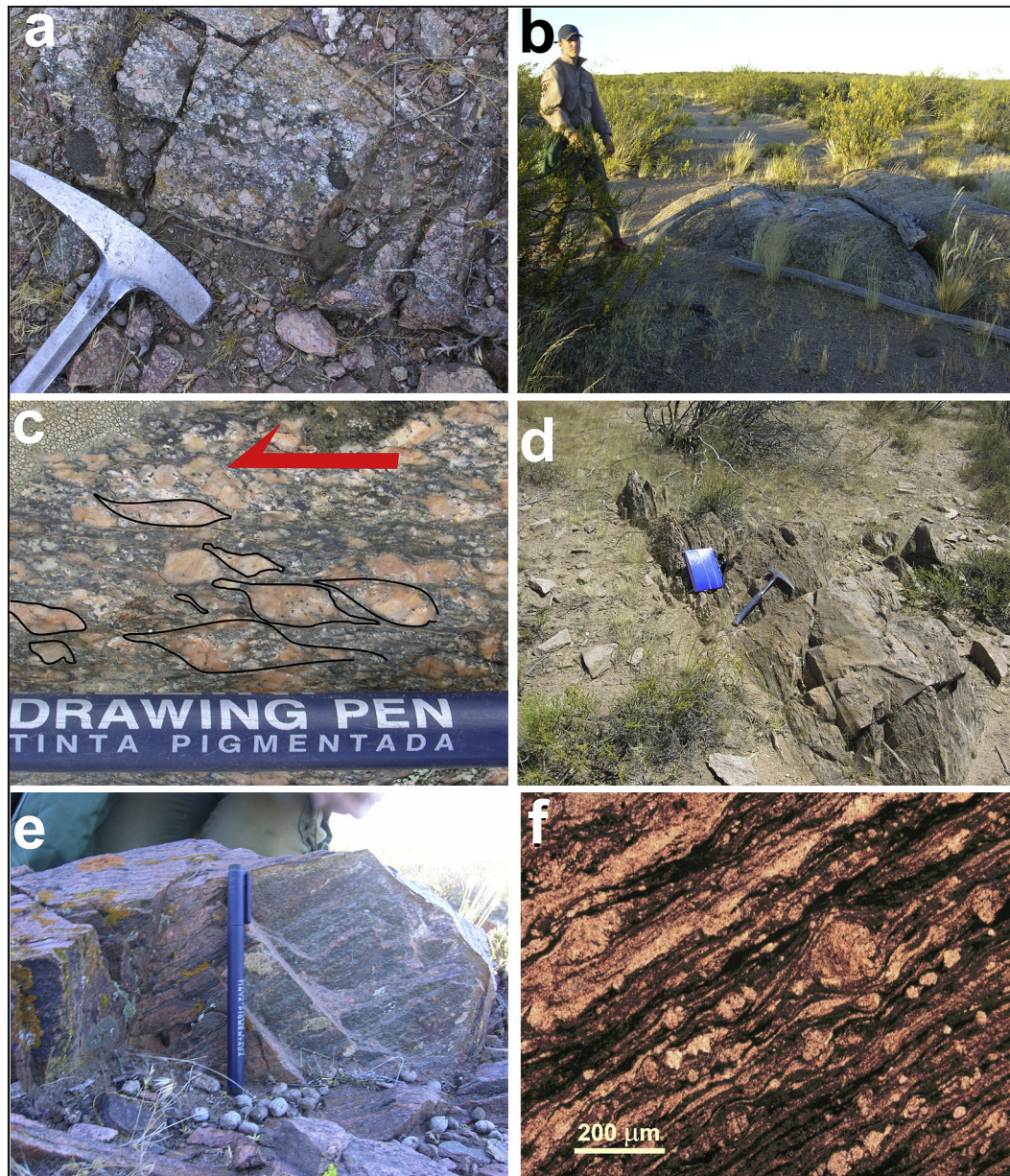


Figure 4. (a) Coarse grained facies of Caita C6 granite, near location depicted in b. (b) Typical outcrops of the Caita C6 granite ~3.5 km north of Estancia La Seña. Most outcrops are of poor quality. (c) Sigmoidal to rounded σ -type porphyroclasts of quartz and K-feldspar in the Caita C6 granite indicating sinistral movement in a wall perpendicular to the foliation plane, along the stretching lineation. (d) Typical outcrops of the Pangaré mylonite, 4 km north of Estancia Pangaré. Steep foliation is dominant in most outcrops of the Pangaré mylonite. (e) Oblique lineations formed by elongated clasts of K-feldspar, quartz and aligned micas in a nearly vertical foliation plane in the Pangaré mylonite, 4 km north of Estancia Pangaré. (f) Photomicrograph of Pangaré mylonite. Rotated clasts of K-feldspar and quartz are wrapped by very fine grained K-feldspar, quartz and calcite ribbons. Scale is 200 μm long. Section cut perpendicular to the foliation plane, along the stretching lineation. Porphyroclasts show sinistral sense of shear.

The second belt, named La Seña mylonite also extends from Sierra Blanca de la Totorá Lineament to Patu C6 Lineament in the area of Estancia La Seña. The rocks pass transitionally eastward to the Caita C6 foliated granite, also defined here. The strikes and longitude of both belts and the close relationship with the Caita C6 granite, as observed in the field, suggest that these rocks were all affected by a common deformational event. Small roof-pendants of metamorphic rocks were found in the foliated granitic rocks.

Both, the Caita C6 granite and the mylonitic belts were intruded by the Alessandrini Complex (Saini-Eidukat et al., 1999) that include granites and rhyolitic and dacitic dikes (Figs. 2 and 3).

Younger rocks in this area are represented by the continental Cretaceous Neuquén Group (Bjerg et al., 1998).

4.1. Metamorphic rocks in La Seña-Pangaré area

Small outcrops interpreted as minor roof-pendants on the Caita C6 granite and composed mainly of amphibolites appear 5 km north of Estancia La Seña (Fig. 3). Primary minerals are hornblende, actinolite, plagioclase, epidote and zircon in a fine granoblastic to nematoblastic texture. Incipient foliation is due to hornblende orientation. Another outcrop was found 2 km north of Estancia

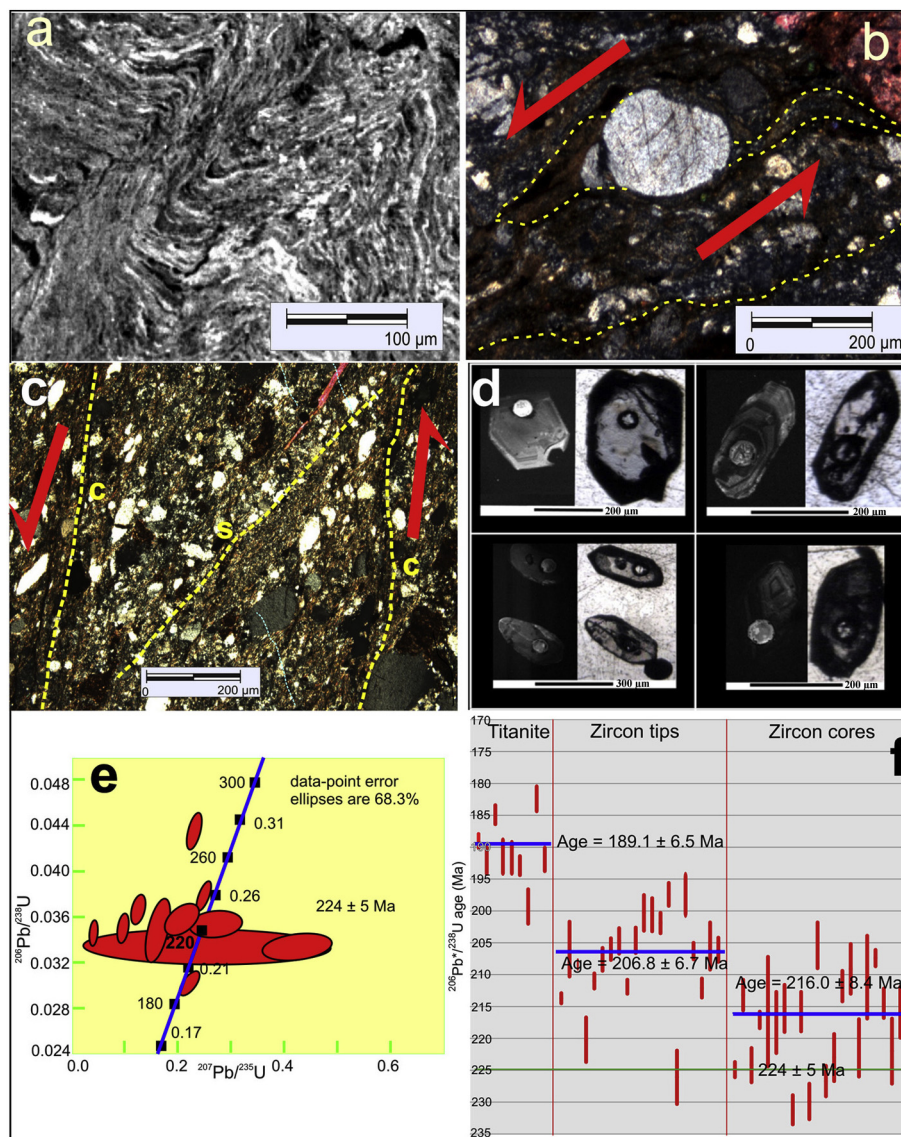


Figure 5. (a) Photomicrograph of a microfolded mylonite (La Seña mylonite). Quartz-K-feldspar bands alternate with bands of dark unidentified material. Scale bar is 100 µm long. Thin section from a sample located 5 km NW of Estancia La Seña. (b) Rotated phenoclast of K-feldspar in La Seña mylonite. Oriented thin section perpendicular to the foliation plane along the stretching lineation. Sample located 3 km south of Cañadón Soledad. (c) S-C structure. Oriented thin section cut perpendicular to the foliation plane along the stretching lineation. Sample located 5 km north of Estancia La Seña. (d) Cathodoluminescence images of typical zircons of the Caita Có granite. They are up to 300 µm long with euhedral morphologies preserving faces and interfacial edges. Laser spots are shown. (e) $^{206}\text{Pb}/^{238}\text{U}$ vs. $^{207}\text{Pb}/^{235}\text{U}$ concordia diagram for the Caita Có granite sample. The curve in the diagram is relative probability trends based on the preferred age derived from individual measurements, which are also shown. $^{206}\text{Pb}/^{238}\text{U}$ ages for values less than 1000 Ma were used. A weighted mean $^{206}\text{Pb}/^{238}\text{U}$ age of 224 ± 5 Ma was obtained in cores, whereas an age of 206 ± 6.7 Ma was obtained from tips. (f) Probabilistic plot of $^{206}\text{Pb}/^{238}\text{U}$ ages displaying three populations: (1) a coherent group of six cores + one tip with age 224 ± 5 Ma; (2) out of 21 cores, a coherent group of 9 shows 216.0 ± 8.4 Ma, and (3) out of 20 tips a group of 8 shows 206.8 ± 6.7 Ma. A group of 5 of 9 titanites shows 189.1 ± 6.5 Ma, which agrees within error with the 192 Ma Rb-Sr age of the Alessandrini Complex.

Pangaré, consisting of micaceous schists blocks included in the foliated granite. Rocks with these characteristics were not previously recognized in the northwestern sector of the North Patagonian Massif.

4.2. The Caita Có granite

The Caita Có granite is a medium- to coarse-grained deformed sheet-like mass (nearly 300 km²) cropping out between Estancias Pangaré and La Seña, and the Sierra Blanca de la Totor Lineament to Patu Có Lineament. The body includes granodioritic, granitic and porphyritic facies, granitic dikes and aplitic veins (Figs. 3 and 4a, b).

The granodioritic facies crops out as small, scattered patches 3 km north of Estancia La Seña. They display a granular, weakly foliated texture composed of twinned plagioclase, hornblende, quartz, K-feldspar and epidote. The granitic facies represents most of the body, whereas the porphyritic facies is common near the La Seña mylonite. The granitic facies (Fig. 4a, b) appears as small rounded hills in a nearly flat area. It commonly contains centimeter long xenoliths of micaceous schists.

The porphyritic facies is small sub-parallel NW–SE trending hills north of Estancia La Seña. Minor outcrops are located north of Estancia Pangaré. K-feldspar phenocrysts (3 mm up to 5 cm long, Fig. 4c) are wrapped by granular zoned plagioclase, quartz, K-feldspar, biotite, muscovite and titanite. Perthites and myrmekites

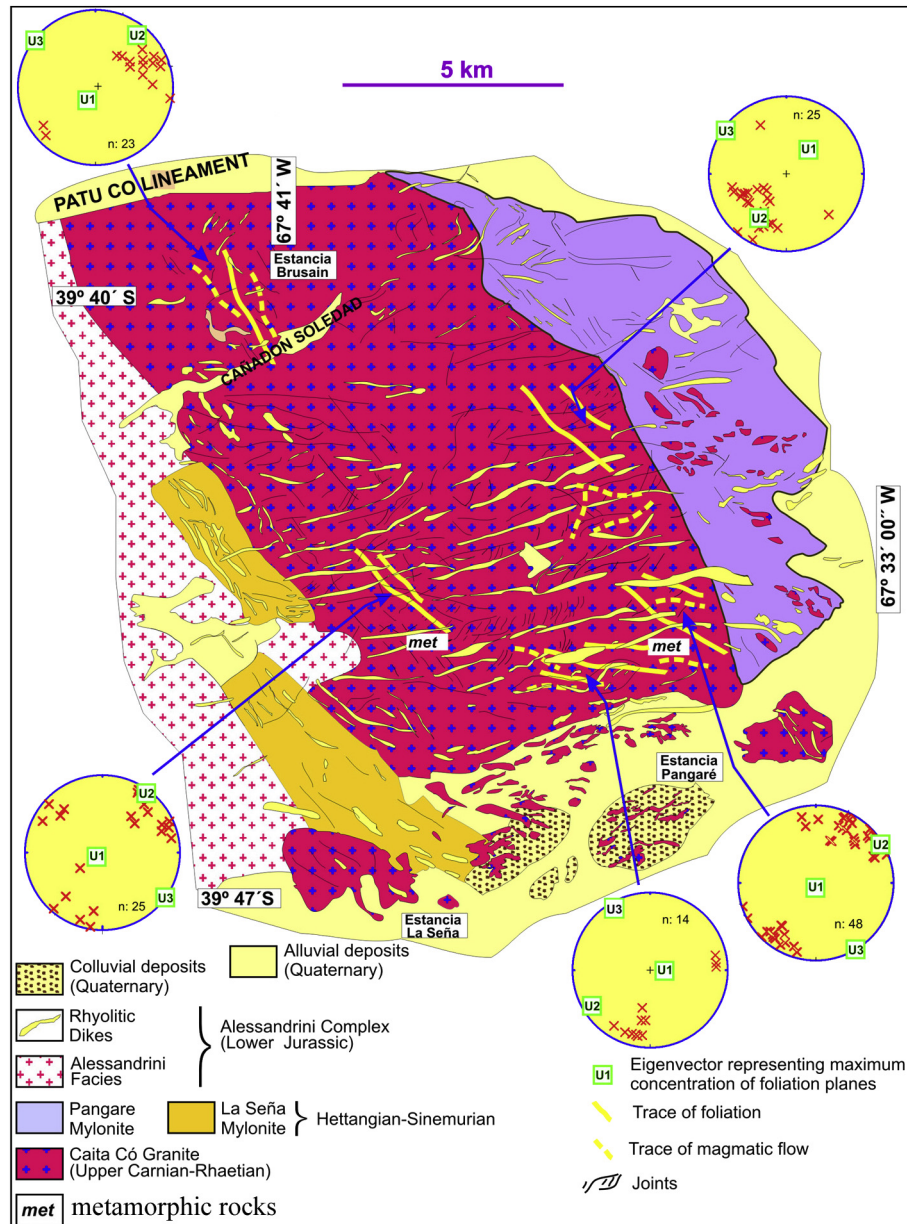


Figure 6. Geological map of the Pangaré and La Señá area showing trace of foliation and magmatic flow in the Caíta Có granite. Lower hemisphere-equal area stereonet of foliation in Caíta Có granite is included. Maximum concentration of foliation planes is represented by eigenvector U1, in a nearly vertical position.

are commonly located at the foliation-parallel borders of feldspar phenocrysts, indicating important grain-boundary diffusion processes, probably enhanced by the presence of interstitial fluids during the deformation.

Westwards of the “large” porphyritic facies, north of Estancia Pangaré there is a medium-size grain porphyritic facies, which consists of twinned plagioclase, perthitic K-feldspar (1 cm long) and quartz phenocrysts immersed in an optically oriented matrix defining a moderate foliation. Myrmekitic textures are common in the borders and cores of K-feldspar. Scarce biotite and muscovite cut the foliation. In some areas, K-feldspar-rich leucogranitic foliated dikes, 10 cm wide, cut the medium-size grained porphyritic facies. These dikes are folded, disrupted by strike-slip faults and cut by dikes of similar composition. Nearly all have a N310°–320° strike. The dip varies between 45° SW/NE to vertical. Foliated and unfoliated granitic and aplitic dikes, striking N310°–325° and up to 15 m wide, cut the other facies.

4.3. Pangaré mylonite

Granitic augen-mylonites, protomylonites, mylonites and ultramylonites form a 15 km long, 400 to 1200 m wide belt from Estancia Pangaré to Patú Co Lineament (Figs. 2 and 3). This belt strikes N310° to N330°, with sub-vertical, NE and SW high-angle dips (Fig. 7). Along strike, the foliation displays some variation in direction with dips from 64° to vertical.

From west to east, different zones of deformation can be recognized. The western zone represents a transition, ~100 m wide, from foliated granites to augen-mylonites, which in turn pass transitionally eastwards to protomylonites, mylonites and ultramylonites.

4.3.1. Augen-mylonites

These rocks show sigmoidal to rounded porphyroclasts of K-feldspar with σ and δ structures. Recrystallized material in tail of

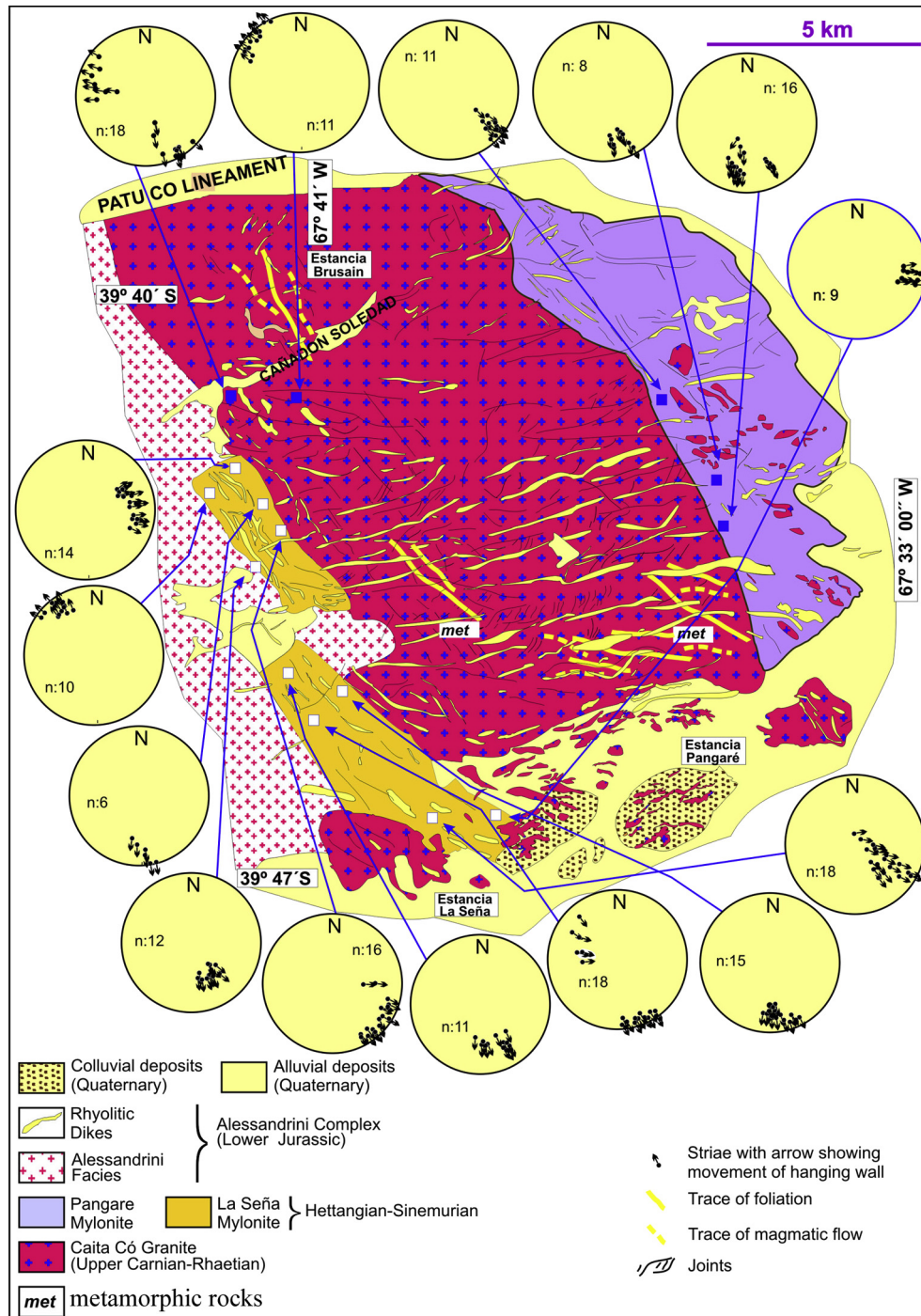


Figure 7. Geological map of the Pangaré and La Seña area showing equal area, lower hemisphere projections of striae with arrow showing movement of the hanging wall of the mylonitic foliation. All calculations were completed with the program "FaultKin 6". Most directions of compression are W–E directed.

porphyroclasts is fine quartz, epidote and chlorite. Porphyroclasts are quartz, single-twinned and myrmekitic K-feldspar and albite-twinned plagioclase. The matrix is microfolded, medium to fine grained and composed of microcrystalline quartz, K-feldspar, plagioclase, biotite, epidote, titanite and allanite. Foliation is marked by development of ribbon quartz and mica fish. Transition to protomylonitic and mylonitic textures is common and indicated in the field as a progressive disappearance of augen K-feldspar and Qz-K-feldspar lenses.

4.3.2. Protomylonites

Diffuse alternating, coarse and thin bands, forming an incipient foliation make up the protomylonites. Coarse bands are composed of quartz, K-feldspar and plagioclase. Quartz, plagioclase and K-feldspar were disrupted to produce porphyroclasts with patchy extinction and fracturing. Biotite-chlorite, epidote-calcite, titanite, allanite and zircon are located in the thin, darker bands. Calcite-epidote veins, K-feldspar and quartz ribbons are warped by biotite parallel to the foliation.

4.3.3. Mylonites

Mylonites constitute the most common lithology of the belt (Fig. 4d–f) and occur in well-defined, high strain zones contiguous to domains of protomylonites. A complete transition between foliated granite, protomylonites and mylonites can be observed in the field. In transitional zones very small, broken K-feldspar crystals inherited from the granitic rock define an incipient foliated, protomylonitic texture. Mylonites display foliation and microfolding with a matrix composed of microcrystalline quartz, calcite and small unidentified minerals. Quartz and perthitic K-feldspar show undulose extinction, fractures and recrystallization tails. The large original mica crystals (biotite and muscovite) are kinked and disrupted to form fine-grained mica-rich bands. Rotated clasts of K-feldspar and quartz indicating sinistral sense of shear are wrapped by very fine grained K-feldspar, quartz and calcite ribbons (Fig. 4f).

4.3.4. Ultramylonites

These are composed by very fine-grained quartz-feldspathic microfolded bands alternating with dark levels of uncertain composition. Only few (<5%) porphyroclasts (<0.1 mm) of quartz, plagioclase and K-feldspar remain. The matrix is fine-grained with a ribbon texture composed of sericite, calcite, microcrystalline quartz and opaque minerals. Microfolding during deformation caused the development of crenulation cleavage with axial planes nearly parallel to the foliation planes. Calcite is crystallized in the hinge zones. Fine-grained quartz, epidote and calcite veins cut the foliation obliquely.

4.4. La Seña mylonite

The La Seña mylonite forms a N310°–320° strike belt, 10 km long and 400–500 m wide, cropping out at the western border of Caíta C6 granite (Figs. 2 and 3). The Alessandrini Complex intrudes the western border of the La Seña mylonite, and fine-grained granitic dikes with a W–E strike cut the mylonites and also the Caíta C6 granite.

The La Seña mylonite is composed of granitic augen-mylonites and mylonites, which display NW–SE strike foliation, dipping with high-angle to the E and W (Fig. 7). The augen-mylonites are composed of up to 7 mm long, porphyroclasts of feldspar, with quartz, biotite and opaque minerals in a fine matrix. Augen porphyroclasts of quartz show sawed borders and are rotated. Biotite can be recognized in the matrix, where it is aligned parallel to quartz ribbons and the foliation. Plagioclase in the matrix exhibits deformed twins. Perthitic K-feldspar develops flame-like and myrmekitic textures that grow during deformation and recrystallization.

The mylonitic rocks are composed of 5% small porphyroclasts of K-feldspar, quartz and plagioclase, wrapped by a fine-grained matrix of quartz and calcite. The matrix shows foliation marked by the orientation of opaque minerals and quartz ribbons. First and second order isoclinal folds with vertical plane axes parallel to the mylonitic foliation were found in several localities. These folds were recognized even on microscopic scale (Fig. 5a).

4.5. Alessandrini Complex

West of the La Seña mylonite crops out non-foliated, equigranular and porphyritic pink granites, granodiorites, and granitic, aplitic and pegmatitic dikes assigned to the Alessandrini Complex (Figs. 2 and 3). The pink to red and coarse granite was named Alessandrini facies, whereas the gray fine-grained granite is known as Cortes facies. These facies were intruded by aplitic and pegmatitic dikes. Rhyolitic and dacitic dikes following NE–SW and E–W

directions intrude the above cited facies. The last event of this igneous complex is the Puesto Mendoza ignimbrites.

Preliminary dating on the Alessandrini facies (Saini-Eidukat et al., 1999) using Rb/Sr on whole rock, feldspar and biotite indicate an age of 192 ± 0.21 Ma. A new Rb/Sr isochrone (Saini-Eidukat et al., 2002) on whole rocks of the Alessandrini, Cortes facies, granodiorites and aplitic dikes yield an age of 195 ± 11 Ma, which agree with the Saini-Eidukat et al. (1999) dating. The rhyolitic and dacitic dikes that cut the intrusive facies of the Alessandrini Complex, as well as the mylonitic belts and the Caíta C6 granite were also dated. A Rb/Sr isochrone yielded an age of 193 ± 13 Ma, with a high value of MSWD (Saini-Eidukat et al., 2002). This age is highly concordant with those obtained in the intrusive facies and suggests a common magmatic history for these rocks.

A fine grained equigranular sample of the Cortés Facies, located north of Cañad6n Soledad at 39°43'S–67°44'W, was analyzed for U–Pb geochronology at the Arizona LaserChron Center, Department of Geosciences, University of Arizona using the procedures described by Gehrels et al. (2008). In this sample a group of zircons give an age of 195 ± 3.1 Ma (Saini-Eidukat et al., 2004). The inherited zircons of this sample yield an age of 223 ± 6 Ma which is equivalent to the Caíta C6 granite.

5. New Geochronological data

5.1. Age of the Caíta C6 granite

A fresh, foliated sample of the Caíta C6 granite collected north of Cañad6n Soledad at 39°41'S–67°42'W was analyzed for geochronology at the Arizona LaserChron Center, Department of Geosciences, University of Arizona using the procedures described by Gehrels et al. (2008). Separated crystals of zircon are typically medium-grained (250 μ m long), show euhedral morphology with magmatic zonation in CL, and preserved faces and interfacial edges. No overgrowths or metamorphic zircons with internal structures were observed (Fig. 5d). Fifty analyses using $^{206}\text{Pb}/^{238}\text{U}$ ages in zircon cores and tips indicated three populations. The oldest, more represented in the cores, yields an age of 224 ± 5 Ma (Fig. 5e and f). A second coherent population that includes cores and tips of zircons indicates an age of 216 ± 8.4 Ma. The younger population, more represented by tips, yields an age of 206 ± 6.7 Ma (Fig. 5f).

A few analyses in titanite give an age of 189 ± 6.5 Ma, possible due to heating related to the intrusion of the Jurassic Alessandrini Complex. See also Table 1. Therefore, the crystallization age is considered to be upper Carnian to Rhaetian.

5.2. Age of La Seña mylonite

No radiometric dating was carried out on the La Seña mylonite. However, field relationships allow to establish its relative age. As indicated in Fig. 3, the western border of the La Seña mylonite shows a sharp, intrusive contact with the Alessandrini facies of this complex. As indicated in section 4.5 the age of this body is between 192 ± 0.21 and 195 ± 11 Ma (Rb/Sr ages, Saini-Eidukat et al., 1999, 2002). The rhyolitic and dacitic dikes of the Alessandrini Complex that cut the mylonitic belt yield an age of 193 ± 13 Ma (Saini-Eidukat et al., 2002). Consequently, the development of the La Seña mylonite must be earlier than Pliensbachian (International Commission on Stratigraphy, 2012). Furthermore, U/Pb dating of the Caíta C6 granite indicates ages between 224 ± 5 and 206 ± 6.7 Ma (upper Carnian–Rhaetian, International Commission on Stratigraphy, 2012). Therefore, the age of the La Seña mylonite and possibly the Pangaré mylonite must be constrained between 206 and 193 Ma (Norian–Sinemurian) (Fig. 8).

Table 1

U–Pb geochronologic analyses of sample BR-2 by Laser-Ablation Multicollector ICP Mass Spectrometry.

Position	U (ppm)	Isotopic ratios							Apparent ages (Ma)						
		$^{206}\text{Pb}_{\text{m}}/^{204}\text{Pb}$	U/Th	$^{207}\text{Pb}^*/^{235}\text{U}$	\pm (%)	$^{206}\text{Pb}^*/^{238}\text{U}$	\pm (%)	Error corr.	$^{206}\text{Pb}^*/^{238}\text{U}$	\pm (Ma)	$^{207}\text{Pb}^*/^{235}\text{U}$	\pm (Ma)	$^{206}\text{Pb}^*/^{207}\text{Pb}^*$	\pm (Ma)	
c	18	5808	20	0.25811	10.12	0.03406	1.83	0.18	215.9	4.0	233	26	411	111	
c	8	4778	7	0.24401	34.75	0.03504	2.27	0.07	222.0	5.1	222	83	219	401	
c	16	6471	40	0.19660	28.98	0.03384	1.07	0.04	214.5	2.3	182	56	218	364	
c	36	6937	3	0.20770	8.20	0.03270	0.64	0.08	207.4	1.3	192	17	1	98	
c	20	5622	5	0.27527	36.85	0.03318	3.02	0.08	210.4	6.5	247	98	610	397	
c	23	7107	4	0.22897	19.98	0.03496	2.00	0.10	221.5	4.5	209	45	75	236	
c	17	4967	3	0.24500	28.00	0.03297	1.82	0.07	209.1	3.9	223	67	367	315	
c	26	5122	3	0.29059	20.71	0.03340	1.11	0.05	211.8	2.4	259	59	712	220	
c	12	3394	5	0.20724	51.13	0.03520	1.63	0.03	223.0	3.7	191	102	185	638	
c	47	9367	3	0.20662	10.08	0.03580	1.02	0.10	226.7	2.4	191	21	235	127	
c	15	5565	4	0.21551	17.83	0.03237	1.72	0.10	205.4	3.6	198	38	113	209	
c	25	15,972	2	0.30805	46.44	0.03630	1.20	0.03	229.9	2.8	273	136	658	498	
c	23	6536	3	0.26035	14.50	0.03404	1.40	0.10	215.8	3.1	235	38	431	161	
c	26	3116	3	0.24360	8.78	0.03651	0.97	0.11	231.2	2.3	221	22	119	103	
c	15	25,004	2	0.23925	18.96	0.03396	1.70	0.09	215.3	3.7	218	45	245	217	
c	12	27,444	2	0.30345	27.50	0.03432	2.17	0.08	217.5	4.8	269	81	746	290	
c	8	43,225	3	0.26066	51.01	0.03405	3.92	0.08	215.8	8.6	235	127	433	567	
c	66	45,716	3	0.26975	5.17	0.03425	0.59	0.11	217.1	1.3	243	14	496	57	
c	26	93,904	7	0.30320	22.91	0.03540	1.20	0.05	224.2	2.7	269	68	678	244	
c	32	161,500	8	0.24234	8.65	0.03363	1.11	0.13	213.2	2.4	220	21	297	98	
c	45	154,559	5	0.29484	9.13	0.03550	0.53	0.06	224.9	1.2	262	27	612	98	
t	33	11,480	3	0.29094	15.34	0.03249	0.92	0.06	206.1	1.9	259	44	773	161	
t	20	5438	4	0.36005	12.44	0.03240	1.77	0.14	205.5	3.7	312	45	1212	121	
t	46	5619	3	0.27851	8.53	0.03344	0.71	0.08	212.1	1.5	250	24	618	92	
t	58	11,916	6	0.22723	5.67	0.03253	0.61	0.11	206.3	1.3	208	13	226	65	
t	50	5025	3	0.23384	6.30	0.03110	1.38	0.22	197.4	2.8	213	15	393	69	
t	95	21,333	17	0.26011	3.23	0.03570	1.82	0.56	226.1	4.2	235	9	322	30	
t	80	9618	3	0.24879	8.33	0.03110	0.90	0.11	197.4	1.8	226	21	530	91	
t	50	12,324	3	0.20431	8.39	0.03182	0.80	0.10	201.9	1.6	189	17	27	100	
t	40	6938	2	0.26202	5.92	0.03160	1.26	0.21	200.6	2.6	236	16	608	63	
t	21	4002	3	0.23304	20.58	0.03157	1.39	0.07	200.3	2.8	213	48	352	232	
t	40	5256	3	0.20804	13.80	0.03225	0.98	0.07	204.6	2.0	192	29	38	165	
t	64	3588	2	0.26878	3.43	0.03342	0.51	0.15	211.9	1.1	242	9	542	37	
t	36	13,772	2	0.22534	15.67	0.03227	0.95	0.06	204.7	2.0	206	35	225	181	
t	52	22,580	3	0.23431	8.17	0.03248	0.80	0.10	206.0	1.7	214	19	300	93	
t	68	3941	3	0.24103	6.10	0.03272	0.86	0.14	207.6	1.8	219	15	347	68	
t	51	25,168	3	0.20669	8.57	0.03327	0.58	0.07	211.0	1.2	191	18	53	104	
t	25	2740	7	0.26127	13.65	0.03474	1.56	0.11	220.2	3.5	236	36	393	152	
t	71	75,128	2	0.23275	9.47	0.03285	0.38	0.04	208.4	0.8	213	22	258	109	
t	18	14,812	3	0.28478	39.54	0.03247	2.05	0.05	206.0	4.3	254	108	729	419	
t	76	28,396	3	0.25895	5.35	0.03370	0.39	0.07	213.7	0.8	234	14	442	59	
s	72	253	0.8	0.19718	4.34	0.03022	0.91	0.21	191.9	1.8	183.9	65	456	51	
s	18	67	0.5	0.31756	7.99	0.02868	0.98	0.12	182.3	1.8	388	-26	NA	NA	
s	20	87	0.5	0.03116	64.01	0.03140	1.31	0.02	199.3	2.7	31	20	NA	NA	
s	29	127	0.4	0.07343	13.11	0.03038	0.77	0.06	192.9	1.5	72	10	-3261	337	
s	59	168	0.7	0.15048	9.13	0.03018	1.19	0.13	191.7	2.3	142	14	-619	124	
s	27	105	0.5	0.03294	40.13	0.03013	1.30	0.03	191.4	2.5	33	13	-15,880	13,892	
s	52	220	0.6	0.18320	3.80	0.02909	0.56	0.15	184.9	1.1	171	7	-20	45	
s	17	80	0.4	-0.04548	40.01	0.03026	1.03	0.03	192.2	2.0	-47	-19	NA	NA	
s	75	317	1.0	0.21667	3.62	0.02975	0.55	0.15	189.0	1.1	199	8	321	41	

 $^{206}\text{Pb}/^{204}\text{Pb}$ is measured ratio. All errors are at the 1 σ level.

Position: c = core of zircon grain, t = tip of zircon grain, s = core of titanite grain. U concentration and U/Th have uncertainties of ~25%.

Decay constants: $^{235}\text{U} = 9.8485 \times 10^{-10}$, $^{238}\text{U} = 1.55125 \times 10^{-10}$, $^{238}\text{U}/^{235}\text{U} = 137.88$.Isotope ratios are corrected for Pb/U fractionation by comparison with standard zircon with an age of 564 ± 4 Ma.Initial Pb composition interpreted from [Stacey and Kramers \(1975\)](#).

6. Fabrics and deformation of the Caita C6 granite, Pangaré and La Seña mylonites

Preliminary calculations of maximum shortening vectors were made with the program “FaultKin 6” written by Allmendinger, Marrett, and Cladouhos ([Marrett and Allmendinger, 1990](#); [Allmendinger et al., 2012](#)).

6.1. Caita C6 granite

The Caita C6 granite ([Fig. 4a](#) and [b](#)) shows a diffuse to strong foliation that records continuous transitions between magmatic fabrics and a clearly foliated tectonic texture. The magmatic fabric

consists of large tabular, aligned euhedral K-feldspar crystals that display twin-growth planes parallel to grain boundaries. Medium-sized to large isolated grains of ilmenite, and allanite/epidote are also aligned together with the K-feldspar crystals. The centimeter-sized K-feldspar phenocrysts have their 010 faces aligned in a nearly horizontal position. Orientation patterns of feldspar phenocrysts, as well as metamorphic xenoliths as shown in [Fig. 3](#), can be used to determine the flow direction.

The diagrams reveal a consistent orientation pattern, where two different structural domains can be distinguished. The first one is predominantly NW–SE to WNW–ESE and appears in the north-western area, near Estancia Brusáin where the average direction measurement is N325°. Similar patterns, including xenoliths

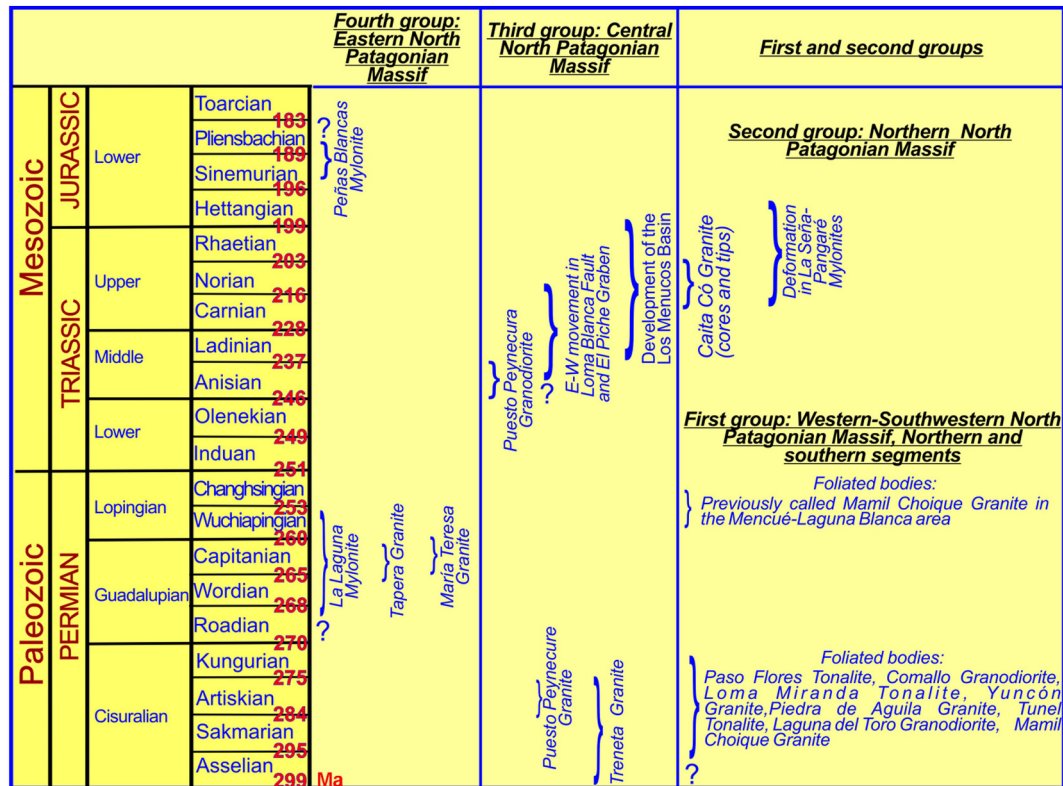


Figure 8. Chronostratigraphic chart displaying Gondwanan ages of emplacement of deformed granitic bodies, mylonitic belts and structural lineaments in northern Patagonia.

orientation can be recognized in the southern part of the area, near Estancia La Seña, north of Estancia Pangaré and close to Pangaré mylonite. There, average directions are N306°, N298°, N290°, N278°, and N262°. The second domain was recorded in only a few localities. It follows NNE–SSW, NE–SW and even E–W directions, mostly detected near and north of Estancia Pangaré. However, a few were recorded near the Pangaré mylonite. A preliminary conclusion regarding these results is that the magmatic flow was predominantly in NW–SE to WNW–ESE directions, not only in the borders of the body, but in areas away from the boundaries.

The foliated textures are defined by oriented plates of biotite, muscovite and sigmoidal clasts of K-feldspars (Fig. 4c) that possibly represent a high-temperature solid-state deformational event. At the microscopic scale, the granite samples show S–C fabric (Berthe et al., 1979), mica fish (Lister and Snoke, 1984) and asymmetric quartz strain shadows around feldspar porphyrocrysts. The quartz crystals have strong undulatory extinction and serrated grain boundaries, both attesting intracrystalline deformation and grain boundary migration recrystallization (Passchier and Trouw, 1996). Kinked biotites, myrmekites and microcline twinning in K-feldspar observed in the samples have been inferred as deformation induced textures (Simpson and Wintsch, 1989; Vernon, 2004).

The diagrams in Fig. 6 show poles of foliation planes and the eigenvectors with U1 representing the maximum concentration of such planes. The subvertical domain (U1) is predominantly along the granitic body. The strike of foliation ranges between NW–SE and WNW–ESE. In most cases U1 is nearly vertical or high angle dips (75° to 88° E and W, see Fig. 6). A second population of foliation planes, represented by U2, display low dip or a nearly horizontal attitude. In the map of Fig. 6 the magmatic flow directions and the foliation trajectories are shown, indicating that both strike parallel to the long axis of the body in most of the analyzed localities. A few exceptions appear near the Pangaré mylonite and north of Estancia Pangaré where E–W and NE–SW directions were recorded.

Most foliation planes are N10°–N70°, dipping 40° to 90° E and W (Fig. 6). The kinematic indicators (deformed K-feldspar crystals) depict sinistral displacements along NW–SE direction (Fig. 4c). Calculation using the software above indicated suggests that principal shortening axes dip 28° in N291° direction and 21° in N279° direction.

6.2. Pangaré mylonite

In hand specimen, the Pangaré mylonites are characterized by a prominent foliation and a moderate lineation (Fig. 4d and e). The lineation is represented by alignment of sericite and muscovite, elongated quartz, and small sigmoidal to rounded σ -type porphyroclasts of quartz and K-feldspar (Fig. 4f). Only a few outcrops with micro and meso folds were found 3 km north of Estancia Pangaré.

In this belt, measurements of lineation and interpretation of kinematic indicators (lunate steps in foliation planes, σ -type porphyroclasts of quartz and K-feldspar) were made on three locations and the results were plotted in the equal area, lower hemisphere projections of Fig. 7, where arrows show direction and sense of movement of the hanging wall.

In the northernmost location foliation planes strike NE, dipping ~40°–80° W, with lineations dipping in the same angles that foliation planes. Lunate steps in foliation planes and deformed porphyroclasts of quartz and K-feldspar indicate movement in the hanging wall in SE direction. Those located 2.5 km south display the same sense of movement. The southernmost location exhibits a south directed movement of the hanging wall with maximum shortening vector dipping 52° in N302° direction. Therefore, in this belt, shortening directions are predominantly NW–SE (Fig. 7).

6.3. La Seña mylonite

Textures and fabrics of the La Seña mylonite suggest metamorphic conditions of medium grade (Passchier and Trouw, 1996).

Relative sense of movement was established using deformed σ -type porphyroclasts of quartz and K-feldspar (Fig. 5b), and lunate steps in the foliation planes. Most of them indicate sinistral movement, although in some areas dextral movement was recorded. In this belt, the rock shows ribbon textures made up by orientation of biotite, muscovite and chlorite flakes, rotated porphyroclasts and strips of calcite. The lineation is recorded by elongated feldspar and quartz clasts and aligned muscovite and sericite. S-C structures were recognized in thin sections cut perpendicular to the foliation planes along the stretching lineation.

The mylonitic foliation is NNW–SSE striking (Fig. 7) with a mean at N300°–N50° and dips highly variable to the SW or NE. In this belt, measurements of lineation and interpretation of kinematic indicators were made on 10 locations and the results were plotted in the equal area, lower hemisphere projections of Fig. 7.

In the northern part of La Seña mylonite, 2 km south of Cañadón Soledad, five different striae populations were measured. In those located northernmost strike of foliation planes population can be grouped as follows: 45% of them vary between N340° and N25°, dipping W, 33% strike N25° to 60°, dipping SE and 25% (n: 6) with strike between N90° and N115°, dipping N (Fig. 7).

In the first, lineations strike 240° to 280° plunging 25° to 48° W with displacements of the hanging wall in east direction. In the second location lineations strike vary between N310°–N330°, plunging SE with movement of the hanging wall to the NW. In the last location striae strike south and dip N to NE with a south directed displacement of the hanging wall. Shortening axes are N–S and predominantly W–E.

One kilometer south measures indicate that foliation planes strike NE and dips NW, whereas lineations dip W or NW, with displacement of the hanging wall in SE direction (Fig. 7). Their maximum shortening was along directions NW–SE and W–E.

In the southern part of La Seña mylonite, measurements located 5 km north of Estancia la Seña show that foliation planes strike NE and E, dipping 40° to 83° W and N. Lineations are located in the foliation planes and strike mostly in N or W directions (Fig. 7). Kinematic indicators (δ and σ porphyroclasts of quartz and K-feldspar, steps on foliation planes, S-C structures in thin sections) show displacements of the hanging walls in south direction with maximum shortening axes in N or NW direction. Near Estancia Pangaré foliation planes strike N and NE, dipping 25° to 85° W, with lineation strikes N240° to 290°. The kinematic indicator recognized in field (steps in foliation planes) shows sinistral displacements. Therefore, in this area maximum shortening axis was located in E–W direction (Fig. 7).

In summary, in the northern portion of this belt, between Cañadón Soledad and a location situated 5 km south of the Cañadón, two maximum directions of shortening were recognized. One population (75%) has direction E–W, whereas the other is NW–SE. In the southern portion of the belt, near Estancia La Seña, two different populations of shortening directions were recognized. One (75%) is W–E and the another is N–S to NW–SE.

7. Discussion

7.1. Deformation of the Caita Có granite

As above indicated, orientation of the metamorphic enclaves and the K-feldspar phenocrysts indicate the existence of magmatic flow in this body (Figs. 3 and 6). The presence of plagioclase crystals undergoing bending (i.e. deformed at a temperature higher than their plasticity threshold), alignment of muscovite and sericite, tail at feldspar clasts imply that high temperature solid-state fabrics overprint magmatic and sub-magmatic structures (Paterson et al., 1989). Some of these microstructures appear to result from a

continuous deformation, from the solidus temperature to moderate temperatures in the solid state (600–500 °C) (Paterson et al., 1989).

The patterns of orientation of the metamorphic enclaves and the K-feldspar (Fig. 3) recognized in this body can be explained by invoking different types of arguments. The first suggests that particles rotate faster when their flat faces are oriented with high angles to the shear plane, and slow down or even stop when their flat faces rotate to small angles with the shear plane parallel to it (Nicolas, 1987). The second argument is related to the assumption that the magmatic flow plane is parallel to the plane of maximum alignment of phenocrysts; grains parallel to the flow plane would reflect the orientation of finite strain, and oblique grains would demonstrate the orientation of a smaller increment of strain (Blumenfeld and Bouchez, 1988). The last argument is based on the different vorticities of rigid particles during non-coaxial flow in a weak matrix (Fernandez et al., 1983). Such different vorticities imply that grains with small aspect ratios are oriented with their flat faces closer to the flow plane than grains with higher aspect ratios.

Accordingly, based on orientation patterns of K-feldspar phenocrysts and metamorphic xenoliths, we conclude that the magma of the Caita Có granite flowed in a NW–SE direction, while solid-state deformation was associated with E–W and NW–SE directions of shortening.

7.2. Emplacement of the Caita Có granite

It is unlikely that the elongated shape of this body (>15 km long, 7 km wide, Figs. 2 and 3) was caused by solid state deformation from an original body with a much smaller axial ratio. Therefore, the pluton most probably intruded as a sheet-like body into an opening pull-apart structure. This can be inferred from the parallelogram-like map outline of the pluton and its boundaries being formed by shear zones (Figs. 3, 6 and 7). Bending of a major, regional, ductile shear zone may have caused the opening of this pull-apart structure.

Some authors have proposed that the root zones of plutons emplaced in a transpressive regime correspond to areas where magma feeders are concentrated (Brown and Solar, 1999; Benn et al., 2000; Rosenberg and Handy, 2005). The root zones are generally sheet-like, associated with shear zones and elongated parallel to the regional structures. The Caita Có granite possibly represents a root zone with strong high temperature solid state deformation and shows the link that exists between a transfer zone of magma and the formation of a shear zone in a transpressive context.

7.3. Deformation of Pangaré and La Seña mylonites

In the Pangaré and La Seña mylonites, the fabric suggests that mylonitic deformation occurred under at least medium grade metamorphic conditions (Passchier and Trouw, 1996). Clearly-defined porphyroclasts of K-feldspar, lenses of Qz-K-feldspar, S-C structures and mica fish support sinistral movement. In La Seña mylonite σ_1 is located in E–W direction, possibly in a subhorizontal position. Field relationships with the Caita Có granite and the Alessandrini Complex indicate that the deformational event lasted between the Carnian and Hettangian times.

7.4. Chronology of the Gondwana deformed granites in the North Patagonian Massif

Deformed granites related with the Gondwanide Orogeny were recognized in many areas of northern Patagonia and can be arranged in four separate groups.

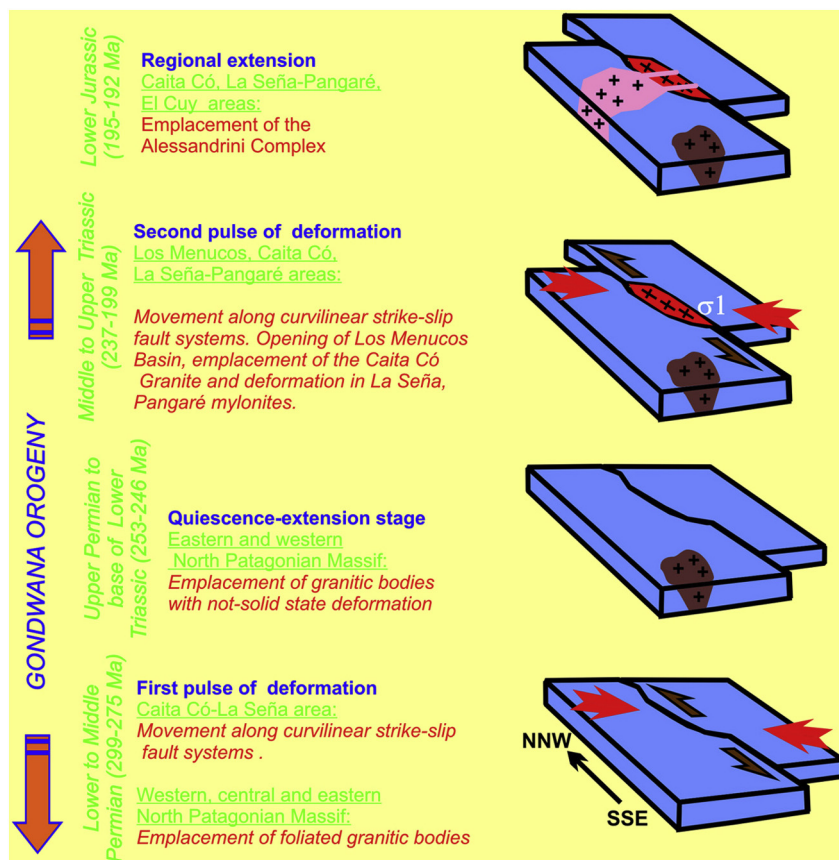


Figure 9. Simplified model of evolution during the Gondwana Orogeny for the Caíta Có-La Seña area, in northern North Patagonian Massif. During lower to middle Permian there was emplacement of deformed granites in several areas, but not in the Caíta Có-La Seña area. Upper Permian and lower Triassic represent a quiescence stage in this region. During middle to upper Triassic a second phase of deformation in central and northern North Patagonian Massif is evident, and includes the opening of the Los Menucos Basin and the emplacement of the Caíta Có granite. In lower Jurassic times the emplacement of the Alessandrini Complex points to the end of the Gondwanide Orogeny.

7.4.1. First group: Western and southwestern North Patagonian Massif

This group is represented by a curvilinear, 300 km long, 100 km wide belt between Mengué and Mamil Choique in the W and SW part of the Massif.

The northern segment of this belt displays a rough SW–NE trend and includes the foliated Paso Flores tonalite, Comallo granodiorite, Yuncón granite, Loma Miranda tonalite, Piedra del Aguila granite and rocks assigned to the former Mamil Choique granite (Figs. 8–10). K/Ar and U/Pb radiometric dating (SHRIMP and bulk analysis in zircon) yield ages between 386.6 ± 5.4 and 272.4 ± 2.2 Ma (Varela et al., 2005; Pankhurst et al., 2006). These rocks were assigned to a magmatic arc developed on continental crust by Varela et al. (2005). Our own unpublished U/Pb ages using ICP-MS in zircon in the previously called Mamil Choique granite, in the Mengué and Laguna Blanca areas indicate ages of ~ 253 Ma.

The radiometric dating of this segment shows a remarkably long (114 Ma) period of plutonism in the western North Patagonian Massif (Fig. 8). However, a careful interpretation of these data indicates that part of these bodies can be related to an earlier event known as Famatinian Orogeny. The absence of detailed mapping, type of deformation, geochemical and geochronology data preclude an adequate separation between the Famatinian and the Gondwanan magmatic cycles (Varela et al., 2005; Pankhurst et al., 2006). Some of the I-type Carboniferous bodies, with initial $^{87}\text{Sr}/^{86}\text{Sr}$ 0.7034–0.7046, located immediately west of the North Patagonian Massif were related by Pankhurst et al. (2006) to a Carboniferous subduction system. Peraluminous S-type leucogranites located in this area yield ages of 314 ± 2 and 318 ± 2 Ma.

According to Pankhurst et al. (2006), these results suggest that in the southwestern part of the North Patagonian Massif an episode of subduction followed by crustal anatexis was developed in the Carboniferous, along a NW–SE direction in the SW border of the Massif.

The southern segment of this belt displays a rough NW–SE trend and includes the Tunel tonalite (295 ± 2 Ma), the Laguna del Toro granodiorite (294 ± 3 Ma), and the Mamil Choique granite (Figs. 8 and 10). According to Pankhurst et al. (2006) these bodies may have been generated during continued deformation, and include rocks with both metaluminous I-type and peraluminous S-type affinities.

7.4.2. Second group: Northern North Patagonian Massif

This group is formed until now only by one deformed body, the Caíta Có granite, which was described above. As indicated, the magmatic flow was SE–NW directed, whereas the solid state deformation, associated with the development of La Seña and Pangaré mylonites seems to be related to near horizontal W–E directed compression (Figs. 7–9). The age of the deformation of the granite seems to be restricted to a 226–206 Ma age (Fig. 8), whereas the mylonitic belts could extend to 199 Ma. The strike of this body is $\sim \text{N}330^\circ\text{--}340^\circ$ and is parallel to the direction of the Lineament “B” described by Gregori et al. (2008).

7.4.3. Third group: Central North Patagonian Massif

In the Yaminué area, the foliated intrusive bodies like the Treneta granite (305 ± 31 Ma, U/Pb zircon; 244 ± 9 Ma, Rb/Sr), Puesto Peynecura granite (281 ± 29 , U/Pb zircon), and Puesto Peynecura

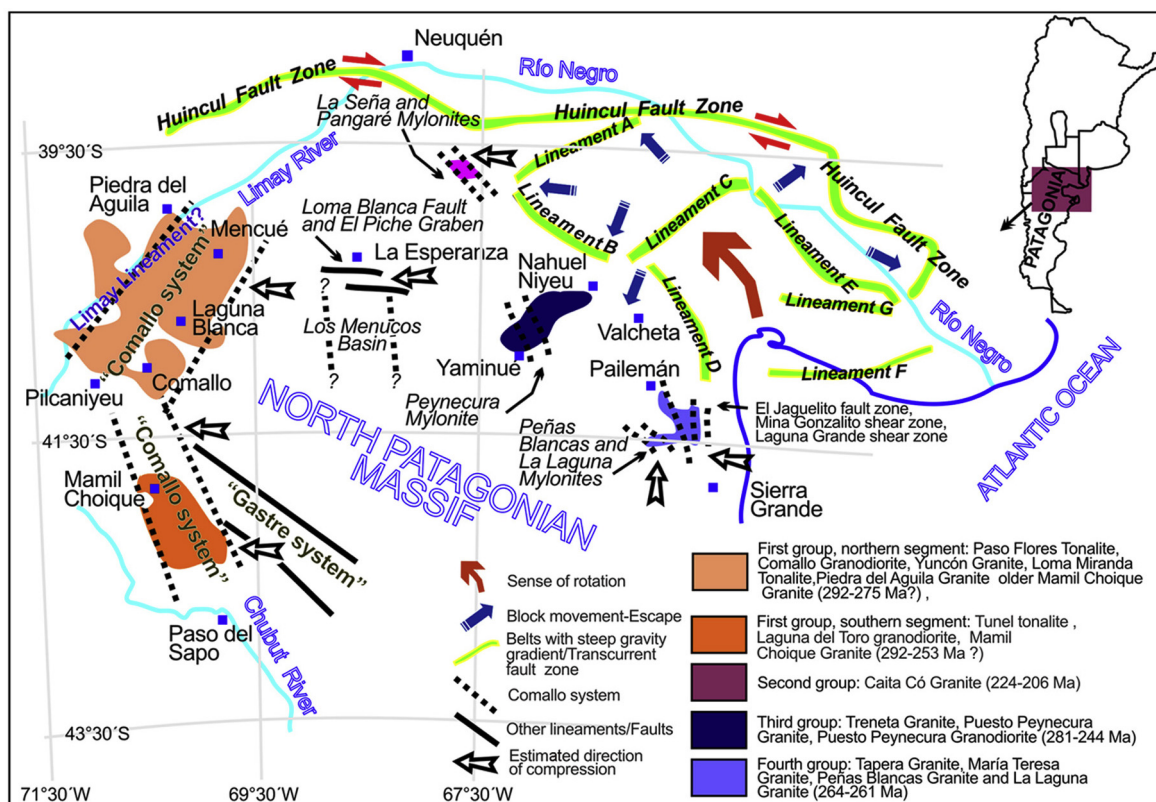


Figure 10. Regional geological sketch of northern Patagonia showing the configuration of regional lineaments, mylonitic belts, block movements, direction of indentation, as well as, belts with steep gravity gradients as described by Gregori et al. (2008, 2013). Fourth groups of deformed granites were differentiated. Estimated direction of compression during the Gondwana Orogeny is depicted.

granodiorite (244 ± 14 Ma, U/Pb zircon), indicate upper Carboniferous to lower Triassic ages (Basei et al., 2002). The last seem to be associated to the Peynecura mylonite that strike $\sim N330^\circ$ (Figs. 8 and 10) being comparable with the strike of rocks in the second group and also with the southern segment of the first group. The ages, using data from zircons ($281\text{--}244$ Ma) is in the range of the intrusives of the first group (Fig. 8).

7.4.4. Fourth group: Eastern North Patagonian Massif

Includes the Tapera granite (264 ± 1.5 Ma, Ar–Ar), María Teresa granite (261 ± 1.4 Ma, Ar–Ar), Peñas Blancas and La Laguna granites (Basei et al., 2002; Grecco and Gregori, 2011), along 50 km in $N330^\circ$ direction, between Pailemán and Arroyo Salado (Figs. 8 and 10). This belt is parallel to lineament “D” of Gregori et al. (2008) and to the El Jagüelito fault zone and other subparallel lineaments (Fig. 9), to which they are apparently related. Most of them are S type granites. According to von Gosen (2002) the Peñas Blancas granite is associated with the Peñas Blancas mylonite, where a N–S deformation was observed.

7.5. Gondwana mylonitic belts, transcurrent shear zones and structural lineaments in the North Patagonian Massif

As indicated by Gregori et al. (2008) the North Patagonian Massif is characterized by the presence of several mylonitic belts and long structural lineaments (Fig. 10). Due to the Tertiary and Quaternary sedimentary cover, the distance which these structures extend and their geometrical configuration is sometimes unknown. In most of them, the age and deformational mechanisms remain unclear. Besides these belts, several more recognized at surface and outlined by steep gravity gradients were found during gravimetric

studies (Kostadinoff et al., 2005; Gregori et al., 2008, 2013). Most of them are coincident in direction with the mylonitic belts earlier cited.

In the eastern North Patagonian Massif, 200 km SE of the studied area, appears a NW–SE-oriented belt of strong gravity gradients (Lineament “D” of Gregori et al., 2008) more than 124 km long (Gregori et al., 2013). The belt is partly coincident with the El Jagüelito fault zone (Fig. 10). This fault zone consists of protoclastic and protomylonitic rocks, with mylonitic lineation dipping $14^\circ\text{--}22^\circ$ in north and northeasterly directions, along the fault zone (Giacosa, 2001). This author assigned the El Jagüelito fault zone to an N–N15° dextral transpressive shear zone, with movement between 270–253 and 188 Ma.

In the same area, González et al. (2008) identified the NNW–SSE Mina Gonzalito shear zone. This N–S strike-slip structure dips $54^\circ\text{--}80^\circ$ to the east and exhibits mylonitic lineation, indicating SSE to NNW transport. Eastwards, González et al. (2008) described the $40^\circ\text{--}60^\circ$ west-dipping Laguna Grande shear zone, which displayed sinistral movement. These structures display a similar orientation and movement as the La Señá and Pangaré mylonites. The El Jagüelito, Mina Gonzalito and Laguna Grande Fault zones are all parallel to Lineament “D” of Gregori et al. (2008), represented by a belt with steep gravity gradients (Fig. 10). As earlier indicated, these fault zones seem to be related to the Tapera and María Teresa granites, with deformation in the middle Permian (261–264 Ma).

Other NW–SE mylonitic belts in this area include the 10 km long Peñas Blancas and La Laguna mylonites described by Giacosa (1996). The first are temporally related to the foliated Jurassic Peñas Blancas granite (Busteros et al., 1998). The age of this body is controversial because it is directly related with the El Jagüelito Fault zone which indicates a Permian age for the deformation. The

second seems to be related to the foliated Permian La Laguna granite intruded by the non-foliated La Verde granite (253 ± 9 Ma; Linares, in [Busteros et al., 1998](#)).

In the central part of the North Patagonian Massif, 120 km SSE, the Peynecura mylonitic belt ([Llambías et al., 2002](#)) is more than 500 m wide, 15 km long, and has a NNW–SSE strike. Although no kinematic data are available, it is supposed that the deformation has occurred between the lower Permian and middle Triassic because it is related to foliated granites of such age ([Fig. 9](#)).

In the La Esperanza area, located 100 km SW, two regional strike-slip systems were recognized by [Corbella \(1975\)](#). The first, called the Loma Blanca fault is a 30 km long E–W curvilinear dextral structure that displaces the Calvo granite (250 Ma; [Pankhurst et al., 2006](#)) by more than 7 km. The second structure, known as El Piche Graben is 80 km long, W–E directed and shows sinistral displacement in plane view ([Fig. 10](#)). This graben cuts the Calvo granite and represents the northern border of Los Menucos Basin. This graben hosts part of the sedimentary pile of the Los Menucos Basin with flora fossil remains of *Pleuromeia corda* ([Labudía et al., 1992](#)).

The movement along both structures must be younger than 250 Ma and coeval or slightly older than the beginning of the Los Menucos Basin (237 Ma) ([Figs. 8 and 10](#)). In the Los Menucos area, located 30 km south of La Esperanza, the Los Menucos Basin constitutes a pull-apart structure ([Labudía and Bjerg, 2005](#)) with its western and eastern borders formed by 330° – 340° lineaments systems extending more than 70 km long. The Los Menucos Basin development lasts between the Ladinian and the Rhaetian (late middle to upper Triassic, [International Commission on Stratigraphy, 2012](#)), according to the flora fossil remains ([Artabe, 1985a,b; Labudía et al., 1992](#)). The time of opening and geometry of the Los Menucos Basin is comparable with the time of emplacement and geometry of the Caita Có granite and La Seña and Pangaré mylonites. Finally, as indicated, the **Comallo Lineament**, which also displays a principally NW–SE trajectory was active during the lower Permian with a W–E directed stress. Therefore, along the North Patagonian Massif many NW–SE structural lineaments, represented by strike-slip faults, mylonites and belts with steep gravity gradients ([Gregori et al., 2008](#)) can be recognized. The younger age of these movements is constrained by the Alessandrini Complex (~ 195 Ma), the Marifil Complex (~ 189 Ma) or equivalent units (Garamilla Formation, 187 ± 2.3 Ma; [Benedini and Gregori, 2013](#)) that are not deformed. The maximum age for the initiation of the deformation is more diffuse, but the foliated granites in the western border of the North Patagonian Massif and in the Puesto Peynecura area indicate an upper Carboniferous–lower Permian age for the beginning of deformation. This stage of deformation was coeval, as indicated by dating of foliated granites, in several areas of the North Patagonian Massif and continues intermittently until the upper Triassic.

Therefore, lineaments “B” and “D” as proposed by [Gregori et al. \(2008, 2013\)](#) are represented by La Seña and Pangaré mylonites, as well as by the El Jagüelito, Mina Gonzalito and Laguna Grande Fault zones. In both areas, movement was active between upper Triassic and lower Jurassic.

7.6. Tectonic events in the Caita Có-La Seña area

According to our observations and regional evidences, the emplacement of the Caita Có granite was related to a succession of tectonic events as depicted in [Fig. 9](#).

A regional strike-slip fault zone was developed in lower to middle Permian times, due to movements related to the indentation tectonics proposed by [Gregori et al. \(2008\)](#). In the Caita Có-La Seña area this event has not direct evidences, but in the western,

eastern and central areas of the North Patagonian Massif this event of deformation was related to the emplacement of deformed granites (see section 7.4 and [Fig. 8](#)). During upper Triassic a period of quiescence seems to be developed in the Caita Có area. For the middle to upper Triassic the central and northern part of the North Patagonian Massif was affected by a second pulse of deformation ([Figs. 8 and 9](#)) that reactivated old strike-slip fault zones allowing the emplacement of the Caita Có granite, as well as the development of the Los Menucos Basin and the mylonitic belts. Finally, during lower Jurassic the undeformed Alessandrini Complex is intruded in the Caita Có granite and the mylonitic belts.

7.7. Model for the Gondwanide Orogeny in northern Patagonia

According to [Gregori et al. \(2008\)](#) the Gondwana Orogeny in northern Patagonia produces a lineament network that defines block systems ([Fig. 10](#)). These structural lineaments are integrated by strike-slip faults, mylonites, and belts with steep gravity gradients related and unrelated to mylonites. The block systems were particularly active during Gondwana times (Permian to Triassic). The geometry of individual blocks controlled the block movements and therefore the development of mylonitic belts and other lineaments.

If the model of indentation-escape tectonics proposed by [Gregori et al. \(2008\)](#) for northern Patagonia is accepted, then the diverse orientation and kinematics of the Gondwana structural lineaments can be explained. The model can clarify not only the diversity of directions in the mylonitic belts but also the presence and orientation of the belts with steep gravity gradients of Gondwana age. Furthermore, the model explains why foliated and non-foliated granites were coevally intruded next to each other in curvilinear regional lineaments dominated by strike-slip movements forming extensional and contractional domains were the intrusive bodies were emplaced.

As a result, in the North Patagonian Massif during the Permian and Triassic times, intraplate deformation generated block movement along mylonitic belts, strike-slips and transcurrent faults represented by steep gravimetric gradient ([Fig. 10](#)).

This deformation is consistent with counterclockwise rotation during Gondwana times southern of the Huincul Fault zone, possibly due to indentation during block transurrence in the North Patagonian Massif ([Gregori et al., 2008](#)). From the above presented evidences an additional conclusion can be drawn. The Gondwana Orogeny presents a first phase of deformation due to fast indentation in the lower and middle Permian, with emplacement of granitic bodies and deformation along regional lineaments in the western, central and eastern part of the North Patagonian Massif. Apparently continues a period of quiescence in some areas of the massif ([Fig. 8](#)), where were emplaced large granitic bodies without solid state deformation. A new phase of deformation, arising in the lower Triassic continues intermittently along the Triassic ([Fig. 9](#)), with the development of the Los Menucos Basin, the emplacement of the Caita Có granite and the deformation in La Seña, Pangaré mylonites ([Fig. 10](#)).

8. Conclusions

The Gondwana Orogeny in northern Patagonia produced curvilinear regional lineaments dominated by strike-slip movements forming extensional and contractional domains where intrusive bodies were emplaced. These domains include belts of mylonites, regional strike-slip fault zones and belts with steep gravimetric gradients. Along these zones foliated granites were coevally emplaced with the deformation. The Gondwana Orogeny

is related to W–E directed compression due to the indentation of blocks in the eastern part of the North Patagonian Massif.

The deformation in the central northern part of the North Patagonian Massif was recorded in the Caita C6 granite and La Seña–Pangaré mylonites. Several structural evidences in those rocks point to an E–W predominantly direction of compression, similar to the direction proposed by Gregori et al. (2008) in the escape tectonic model for northern Patagonia.

Deformation occurred during the lower and middle Permian and later in the Triassic.

This period of deformation seems to last during Permian–Triassic times, with stages of quiescence during the upper Permian. At that time, undeformed granitic bodies were intruded. This tectonic model was active in the north and central zones of the North Patagonian Massif because the temporary and geometric similarities with the Los Menucos Basin and tectonic lineaments of this age. In the north-eastern part of the North Patagonian Massif, tectonic lineaments with directions of movement and ages of movements similar to the La Seña–Pangaré structure represent its continuity. Therefore, the escape tectonic model affected not only the eastern part of the North Patagonian Massif, if not the central and northern part of this region.

Acknowledgments

This study is part of the research project “Configuración Geológica y Geodinámica del sector central de la Comarca Nordpatagónica, Argentina” (24/H100) granted by the Universidad Nacional del Sur, and “La Orogenia Gondwánica en el sector central de la Comarca Nordpatagónica” (11420090100108) granted by CONICET. We would like to thank the people of the El Cuy locality, as well as the puesteros and Sotera, and Mollo families, that allowed us access to their lands, gave us shelter and helped throughout the many field trips. We are also deeply grateful for the comments and suggestions made by an anonymous reviewer and the Associated Editor Dr. N. Roberts, who provided a detailed critique of the manuscript which considerably improved its quality.

Appendix A. Supplementary data

Supplementary data related to this article can be found at <http://dx.doi.org/10.1016/j.gsf.2015.06.002>.

References

- Allmendinger, R.W., Cardozo, N.C., Fisher, D., 2012. *Structural Geology Algorithms: Vectors & Tensors*. Cambridge University Press, Cambridge.
- Artabe, A., 1985a. Estudio sistemático de la taoflora triásica de Los Menucos, provincia de Río Negro. Parte I. Sphenophyta, Filicophyta y Pteridospermophyta. *Ameghiniana*, Revista de la Asociación Paleontológica Argentina 22 (1–2), 3–22.
- Artabe, A., 1985b. Estudio sistemático de la taoflora triásica de Los Menucos, provincia de Río Negro. Parte II. Cycadophyta, Ginkgophyta y Coniferophyta. *Ameghiniana*, Revista de la Asociación Paleontológica Argentina 22 (3–4), 159–180.
- Basei, M.A.S., Varela, R., Sato, A.M., Siga Jr., O., Llambías, E.J., 2002. Geocronología sobre rocas del Complejo Yaminué, Macizo Norpatagónico, Río Negro, Argentina. CDROM.
- Benedini, L., Gregori, D.A., 2013. Significance of the Early Jurassic Garamilla formation in the western Nordpatagonian Massif. *Journal of South American Earth Sciences* 45, 259–277.
- Benn, K., Odonne, F., Lee, S.K.Y., Darcovich, K., 2000. Analogue scale models of pluton emplacement during transpression in brittle and ductile crust. *Transactions of the Royal Society of Edinburgh: Earth Sciences* 91 (1/2), 111–121.
- Berthe, D., Choukroune, P., Jegouzo, P., 1979. Orthogneiss, mylonite and non-coaxial deformation of granites: the example of the South Armorican Shear Zone. *Journal Structural Geology* 1, 31–42.
- Bjerg, E.A., Gregori, D.A., Labudía, C.H., 1998. Geología y estratigrafía de la región de El Cuy, Comarca Nordpatagónica, provincia de Río Negro, República Argentina. *Revista de la Asociación Geológica Argentina* 52, 387–399.
- Blumenfeld, P., Bouchez, J.L., 1988. Shear criteria in granite and migmatite deformed in the magmatic and solid states. *Journal of Structural Geology* 10, 361–372.
- Brown, M., Solar, G.S., 1999. The mechanism of ascent and emplacement of granite magma during transpression: a syntectonic granite paradigm. *Tectonophysics* 312, 1–33.
- Buggisch, W., 1987. Stratigraphy and very low grade metamorphism of the Sierras Australes de la Provincia de Buenos Aires (Argentina) and implications in Gondwana correlation. *Zentralblatt für Geologie und Paläontologie I*, 819–837.
- Busteros, A., Giacosa, R., Lema, H., Zubia, M., 1998. Hoja Geológica 4166–IV Sierra Grande. Provincia de Río Negro. Programa nacional de Cartas Geológicas de la República Argentina 1: 250.000. In: Boletín, 241. Segemar, Buenos Aires, 75 pp.
- Caminos, R., 1983. Descripción Geológica de las Hojas 39g, Cerro Tapiluke y 39h, Chipauquil, provincia de Río Negro. Servicio Geológico Nacional, (inédito), 41 pp., Buenos Aires.
- Chernicoff, C.J., Santos, J.O.S., Zappettini, E.O., McNaughton, N.J., 2008. Zircon U–Pb SHRIMP Dating of Lower Paleozoic Parashists at Sierra de Lonco Vaca, La Pampa province, Argentina. 6th South American Symposium on Isotope Geology, San Carlos de Bariloche. Proceedings CD-ROM.
- Coira, C., Nullo, F., Proserpio, C., Ramos, V.A., 1975. Tectónica del basamento de la región occidental del Macizo Nordpatagónico (Prov. de Río Negro y Chubut). *Revista Asociación Geológica Argentina* 30, 361–384.
- Corbella, H., 1975. Hallazgo de un complejo alcalino vinculado a megatrazas de fracturas corticales en la sierra de Queupuniyeu, Macizo Nordpatagónico, provincia de Río Negro, Argentina. 2° Congreso Ibero-americano de Geología Económica. Actas 4, 45–68 (Buenos Aires).
- Dalla Salda, L.H., Cingolani, C., Varela, R., 1991. El basamento pre-andino ígneo-metamórfico de San Martín de los Andes, Neuquén. *Revista de la Asociación Geológica Argentina* 46, 223–234.
- Dalla Salda, L.H., Varela, R., Cingolani, C., Aragón, E., 1994. The Rio Chico Paleozoic Crystalline Complex and the evolution of Northern Patagonia. *Journal of South American Earth Sciences* 7, 377–386.
- Fernandez, A., Febesse, J.L., Mezure, J.F., 1983. Theoretical and experimental study of fabrics developed by different shaped markers in two-dimensional simple shear. *Bulletin Societe Géologique France* 7, 319–326.
- Gehrels, G.E., Valencia, V., Ruiz, J., 2008. Enhanced precision, accuracy, efficiency and spatial resolution of U–Pb ages by laser ablation-multicollector-inductively coupled plasma-mass spectrometry. *Geochimistry, Geophysics, Geosystems* 9, Q03017. <http://dx.doi.org/10.1029/2007GC001805>.
- Giacosa, R., 1996. Zonas de cizalla frágil-dúctil en el sector oriental del Macizo Nordpatagónico. 13 Congreso Geológico Argentino (Buenos Aires). Actas 2, 395.
- Giacosa, R., 2001. Zonas de cizallas Neopaleozoicas en el sector oriental del Macizo Nordpatagónico. *Revista de la Asociación Geológica Argentina* 56, 131–140.
- González, P.D., Poiré, D., Varela, R., 2002a. Hallazgo de trazas fósiles en la Formación El Jagüelito y su relación con la edad de las metasedimentitas, Macizo Nordpatagónico Oriental, Provincia de Río Negro. *Revista de la Asociación Geológica Argentina* 57, 35–44.
- González, P.D., Sato, A., Basei, M.A., Vlach, S., Llambías, E., 2002b. Structure, Metamorphism and Age of the Pampean-Famatinian Orogenies in the Western Sierra de San Luis. 15° Congreso Geológico Argentino 2, pp. 51–56 (El Calafate, Santa Cruz).
- González, P., Varela, R., Sato, A.M., Campos, H., Greco, G., Nailpauer, M., Llambías, E., García, V., 2008. Metamorfismo regional ordovícico y estructura de la ecinita El Jagüelito al SO de Sierra Grande, Río Negro. XVII Congreso Geológico Argentino, Jujuy, Actas, pp. 849–850.
- González, P.D., Tortello, M.F., Damborenea, S.E., 2011. Early Cambrian archaeocyathan limestone blocks in low-grade meta-conglomerate from El Jagüelito Formation (Sierra Grande, Río Negro, Argentina). *Geologica Acta* 9 (2), 159–173.
- Grecco, L.E., Gregori, D.A., Rapela, C.W., Pankhurst, R.J., Labudía, C.H., 1994. Per-aluminous Granites in the Northeastern Section of the North Patagonian Massif, pp. 1354–1359, 7th Congreso Geológico Chileno.
- Grecco, L.E., Gregori, D.A., 2011. Geoquímica y geocronología del Complejo Plutónico Pailamán, Comarca Nordpatagónica, provincia de Río Negro. In: Leanza, Franchini, Impicini, Pettinari, Sigismondi, Pons, Tunik (Eds.), Actas del XVIII Congreso Geológico Argentino, p. 91 (Neuquén, Argentina).
- Gregori, D.A., Bjerg, E.A., Saini-Eidukat, B., 2000. New Insights on the Jurassic Granites from Somoncuro Region. Patagonia, Argentina. XVII. Simposio sobre la Geología de Latinoamérica. Profil 18, p. 47. Stuttgart, Germany.
- Gregori, D.A., Kostadinoff, J., Strazzere, L., Raniolo, A., 2008. Tectonic significance and consequences of the Gondwanide orogeny in northern Patagonia, Argentina. *Gondwana Research* 14, 429–450.
- Gregori, D.A., Kostadinoff, J., Alvarez, G.L., Raniolo, A., Strazzere, L., Martinez, J.C., Barros, M., 2013. Preandean Geological Configuration of the Eastern North Patagonian Massif. *Geoscience Frontiers, Argentina*, pp. 693–708.
- International Commission on Stratigraphy, 2012. *International Stratigraphic Chart*.
- Keidel, J., 1916. La geología de las sierras de la provincia de Buenos Aires y sus relaciones con las montañas de Sud Africa y los Andes. Dirección General de Minas, Geología e Hidrología, Buenos Aires, Anales 9, p. 78.
- Keidel, J., 1925. Sobre la estructura tectónica de las capas petrolíferas en el oriente del territorio del Neuquén. Dirección General de Minas, Geología e Hidrología, sección Geología, Buenos Aires, Publicación 8, p. 67.
- Kostadinoff, J., Gelós, E.M., 1994. Análisis de las mediciones gravimagnéticas realizadas entre El Fuerte y arroyo Verde, provincia de Río Negro. *Revista de la Asociación Geológica Argentina* 49, 19–25.
- Kostadinoff, J., Labudía, C.H., 1991. Algunas características del basamento en la desembocadura del Río Negro a partir de datos gravimagnéticos. *Revista de la Asociación Geológica Argentina* 46, 173–180.

- Kostadinoff, J., Schillizzi, R.A., 1988. Anomalías gravimagnéticas del litoral patagónico entre Arroyo Verde y el río Chubut. *Revista de la Asociación Geológica Argentina* 43 (1), 80–90.
- Kostadinoff, J., Schillizzi, R.A., 1996. Características geofísicas del litoral atlántico entre el río Chubut y puerto Camarones, provincia del Chubut. *Revista de la Asociación Geológica Argentina* 51 (4), 35–44.
- Kostadinoff, J., Gregori, D.A., Raniolo, L.A., 2005. Configuración geofísica–geológica del sector Norte de la provincia de Río Negro. *Revista de la Asociación Geológica Argentina* 60, 368–376.
- Labudía, C.H., Bjerg, E.A., 1994. Geología del sector oriental de la Hoja Bajo Hondo, provincia de Río Negro. *Revista de la Asociación Geológica Argentina* 49 (3–4), 284–296 (Buenos Aires).
- Labudía, C.H., Bjerg, E.A., 2005. Geología del Grupo Los Menucos, Comarca Nordpatagónica, Argentina, 16° Congreso Geológico Argentino, Actas 1, pp. 233–238 (La Plata).
- Labudía, C.H., Artabe, A.E., Morel, E., Bjerg, E.A., Gregori, D.A., 1992. El género *Pleuromeia* Corda (Lycophyta, *Pleuromiaceae*) en sedimentitas triásicas de Coli Niyeu, provincia de Río Negro, Argentina. *Ameghiniana. Revista de la Asociación Paleontológica Argentina* 29 (3), 195–199.
- Linares, E., 1994. Informe sobre dataciones radimétricas potasio–argón. Informes 3337, 3338 y 3339. INGEIS, Buenos Aires (inédito).
- Lister, G.S., Snoke, A.W., 1984. S-C mylonites. *Journal of Structural Geology* 6, 617–638.
- Llambías, E.J., Rapela, C.W., 1984. Geología de los Complejos Eruptivos de la Esperanza, Provincia de Río Negro. *Revista de la Asociación Geológica Argentina* 39, 220–243.
- Llambías, E.J., Varela, R., Basei, M., Sato, A.M., 2002. Deformación y metamorfismo neopaleozoico en Yaminué, Macizo Nordpatagónico (40°50'S, 67°40'W): su relación con la fase orogénica San Rafael y el arco de los Gondwánides, p. 6, 15 Congreso Geológico Argentino. El Calafate, CDROM, Article 153.
- Marrett, R.A., Allmendinger, R.W., 1990. Kinematic analysis of fault-slip data. *Journal of Structural Geology* 12, 973–986.
- Nicolas, A., 1987. *Principles of Rock Deformation*. Riedel Publishing Company, New York.
- Pankhurst, R.J., Rapela, C.W., Fanning, C.M., 2001. The Mina Gonzalito Gneiss: Early Ordovician Metamorphism in Northern Patagonia, 3rd South American Symposium on Isotope Geology, Pucón, Chile. CD-ROM. SENARGEOMIN, Santiago, pp. 604–607.
- Pankhurst, R.J., Rapela, C.W., Fanning, C.M., Márquez, M., 2006. Gondwanide continental collision and the origin of Patagonia. *Earth-Science Reviews* 76, 235–257.
- Passchier, C.W., Trouw, R.A., 1996. *Microtectonics*. Springer-Verlag, Berlin.
- Paterson, S.R., Vernon, R.H., Tobisch, O.T., 1989. A review of criteria for the identification of magmatic and tectonic foliations in granitoids. *Journal of Structural Geology* 11 (3), 349–363.
- Ramos, V.A., 1975. Geología del sector oriental del Macizo Nordpatagónico entre Aguada Capitán y Mina Gonzalito, Provincia de Río Negro. *Revista de la Asociación Geológica Argentina* 30, 274–285.
- Ramos, V.A., 1984. Patagonia: Un continente paleozoico a la deriva? 9 Congreso Geológico Argentino, Actas 2, pp. 311–325.
- Ramos, V.A., 2008. Patagonia: a Paleozoic continent adrift? *Journal of South American Earth Sciences* 26, 235–251.
- Rapela, C.W., Caminos, R., 1987. Geochemical characteristics of the Upper Paleozoic magmatism in the Eastern sector of the North Patagonian Massif. *Revista Brasileira Geociências* 17, 535–543.
- Rapela, C.W., Díaz, G.F., Franzese, J.R., Alonso, G., Benvenuto, A.R., 1991. El Batolito de la Patagonia central: evidencias de un magmatismo triásico–jurásico asociado a fallas transcurrentes. *Revista Geológica de Chile* 18 (2), 121–138 (Santiago de Chile).
- Rapela, C.W., Llambías, E.J., 1985. Evolución magmática y relaciones regionales de los complejos eruptivos de La Esperanza, provincia de Río Negro. *Revista de la Asociación Geológica Argentina* 40, 4–25.
- Rapela, C.W., Pankhurst, R.J., Harrison, S.M., 1992. Triassic “Gondwana” granites of the Gastre district, North Patagonian Massif. *Transactions of the Royal Society of Edinburgh. Earth Sciences* 83, 291–304.
- Rapela, C.W., Pankhurst, R.J., Llambías, E.J., Labudía, C., Artabe, A., 1996. “Gondwana” Magmatism of Patagonia: Inner Cordilleran Calc-alkaline Batholiths and Bimodal Volcanic Province. Third International Symposium on Andean Geodynamics, St.-Malo, France, Résumés étendus, ORSTOM, Paris, pp. 791–794.
- Rapela, C.W., Pankhurst, R.J., Fanning, C.M., Grecco, L.E., 2003. Basement Evolution of the Sierra de la Ventana Fold Belt: New Evidence for Cambrian Continental Rifting Along the Southern Margin of Gondwana. *Journal of the Geological Society, London* 160, pp. 613–628.
- Rosenberg, C.L., Handy, M.R., 2005. Experimental deformation of partially melted granite revisited: implications for the continental crust. *Journal of Metamorphic Geology* 23, 19–28.
- Saini-Eidukat, B., Bjerg, E.A., Gregori, D.A., Beard, B., Johnson, C., 1999. Jurassic Granites in the Northern Portion of the Somoncuro Massif. Río Negro Province, Argentina. 14 Congreso Geológico Argentino, pp. 175–177.
- Saini-Eidukat, B., Migueles, N., Gregori, D.A., Bjerg, E.A., Beard, B., Gehrels, G., Johnson, C., 2002. The Alessandrini Complex: Early Jurassic Plutonism in Northern Patagonia, Argentina, 15 Congreso. Geológico Argentino, pp. 253–258.
- Saini-Eidukat, B., Beard, B., Bjerg, E.A., Gehrels, G., Gregori, D.A., Johnson, C., Migueles, N., Vervoort, J.D., 2004. Rb-Sr and U-Pb age systematics of the Alessandrini Silicic Complex and related mylonites, Patagonia, Argentina. *Geological Society of America Annual Meeting Abstracts with Programs* 36, 222.
- Simpson, C., Wintsch, R.P., 1989. Evidence for deformation-induced K-feldspar replacement by myrmekite. *Journal Metamorphic Geology* 7, 261–275.
- Stacey, J.S., Kramers, J.D., 1975. Approximation of Terrestrial Lead Isotope Evolution by a 2-Stage Model. *Earth and Planetary Science Letters* 26 (2), 207–221.
- Tickyj, H., Llambías, E.J., Melchor, R.N., 2002. Ordovician rocks from La Pampa Province, Argentina. In: Aceñolaza, F.G. (Ed.), *Aspects of the Ordovician System in Argentina, Serie Correlación Geológica*, vol. 16. Instituto Superior de Correlación Geológica, Tucumán, pp. 257–266.
- Varela, R., Cingolani, C., Sato, A., Dalla Salda, L., Brito Neves, B.B., Basei, M.A.S., Siga Jr., O., Teixeira, W., 1997. Proterozoic and Paleozoic Evolution of Atlantic Area of North Patagonian Massif Argentina. *South American Symposium on Isotope Geology (Sao Paulo/Brazil, June 15–18, 1997)*, pp. 326–329. Extended Abstracts.
- Varela, R., Basei, M.A.S., Sato, A.M., Sita Jr., O., Cingolani, C.A., Sato, K., 1998. Edades isotópicas Rb/Sr y U/Pb en rocas de Mina Gonzalito y Arroyo Salado. Macizo Nordpatagónico Atlántico, Río Negro, Argentina, 10 Congreso Latinoamericano de Geología and 5 Congreso Nacional de Geología Económica, 1, pp. 71–76.
- Varela, R., Basei, M.A.S., Cingolani, C.A., Siga Jr., O., Passarelli, C.R., 2005. El basamento cristalino de los Andes Norpatagónicos en Argentina: geocronología e interpretación tectónica. *Revista Geológica de Chile* 32 (2), 167–187.
- Varela, R., Sato, K., Gonzalez, P.D., Sato, A.M., Basei, M.A.S., 2009. Geología y geocronología Rb-Sr de granitoides de Sierra Grande. Provincia de Río Negro. *Revista de la Asociación Geológica Argentina* 64 (2), 275–284.
- Vernon, R., 2004. *A Practical Guide to Rock Microstructure*. Cambridge University Press, Cambridge.
- von Gosen, W., 2002. Polyphase structural evolution in the northeastern segment of the North Patagonian Massif (southern Argentina). *Journal of South American Earth Sciences* 15, 591–623.